Investigation of the role of FXR1 and SLFN11 in cellular response to genotoxic stress

Qi Fei

Content

Abstract

Various biological responses occur when cells are exposed to endogenous and exogenous stress such as DNA damage, replication stress, and oxidative stress. To maintain genome stability, mammalian cells have developed intricate molecular network including DNA damage response (DDR), replication stress response as well as the oxidative stress response. Defects in these responses lead to several human diseases, such as neurodegeneration disorder and cancer, therefore elucidating the mechanism of these stress responses and function of related genes is crucial for understanding not only the pathophysiological mechanisms of how disease progress but also for developing a novel therapeutic modality. To gain novel insights regarding these disorders and mechanisms, I focused on MRE11, which is an activator for a critical DDR enzyme ATM kinase, and SLFN11, which is known to accelerate chemotherapeutic response.

In chapter 2, I examined whether MRE11 participates in ATM activation during oxidative stress. Both Ataxia-telangiectasia (AT) and MRE11-defective Ataxia-telangiectasia-like disorder (ATLD) patients show progressive cerebellar ataxia because of neurodegeneration. ATM, mutated in AT, can be activated in response to oxidative stress as well as DNA damage, which could be causal for neurodegeneration. However, the role of MRE11 in oxidative stress responses has not been defined. I discovered that MRE11, but not NBS1 and RAD50 (these are components of the MRE11 complex), are indispensable for ROS-induced ATM activation. I also identified FXR1 as a novel MRE11-binding partner by mass spectrometry. FXR1 could bind with MRE11 and showed that both localize to the cytoplasm. Notably, both MRE11 and FXR1 partly

localize to the mitochondria, which are the major generators of ROS. The contribution of FXR1 to DNA damage response seemed minor and limited to homologous recombination (HR) repair, since depletion of FXR1 perturbed chromatin association of HR repair factors and sensitized cells to camptothecin. During oxidative stress, depletion of FXR1 by siRNA reduced oxidative stress responses and increased the sensitivity to pyocyanin, a mitochondrial ROS inducer. Collectively, these findings suggest that MRE11 and FXR1, as a cytoplasmic complex, contribute to the activation of ATM kinase and cellular defense against mitochondrial ROS.

In chapter 3, I examined a role of SLFN11, a member of the long-form SLFN family, in replication stress response. SLFN11 now attracts attentions from cancer researchers since its expression impacts cell fate decisions following chemotherapy. Although SLFN11 harbors the N-terminal ribonuclease (RNase) domain and the C-terminal helicase/ATPase domain, how these domains contribute to the mechanisms of chemotherapeutic response remains poorly understood. Our lab has previously reported that SLFN11 accelerates stalled fork degradation in response to DNA damage and replication stress in a manner dependent on the helicase domain. To clarify the role of RNase domain in SLFN11, I expressed wild-type and mutated on RNase domain of SLFN11 into previously generated *SLFN11*-defective HAP1 cells. I found that the RNase domain mutant was still able to suppress DNA damage tolerance and destabilize the stalled replication forks. I next found the fork degradation is dependent on both DNA2 and Mre11 nuclease, but not on FXR1. Unexpectedly, I observed that the exogenous expression of not only the RNase-deficient but also wild-type SLFN11 downregulated the protein levels of ATR kinase, which is a critical regulator for replication stress response. Finally, I clarified that ATR inhibitor treatment accelerated the stalled fork

degradation. Collectively, these results supported the view that a critical role of SLFN11 in cancer chemotherapy may involve the regulation of ATR levels, and SLFN11 may emerge as a novel modifier of ATR function.

In conclusion, the functional analyses of FXR1 and SLFN11 have provided novel insights in regulation of critical kinases in DNA damage response and replication stress. These results deepened current understanding of the mechanism of cellular response to genotoxic stress in diseases, such as cancer and neurodegenerative disorders.

Abbreviations

AT	Ataxia-telangiectasia
ATLD	Ataxia-telangiectasia-like disorder
ATM	Ataxia-Telangiectasia mutated
ATR	ATM-and Rad3-related
ATRIP	ATR-interacting protein
BER	Base excision repair
BRAC2	Breast cancer susceptibility 2
CHK1	Checkpoint kinase 1
CHK2	Checkpoint kinase 2
CPT	Camptothecin
DDA	DNA damage agents
DDR	DNA damage response
DNA-PKcs	DNA-dependent protein kinase catalytic subunit
DSB	DNA double-strands break
dsDNA	Double strands DNA
EXO1	Exonuclease 1
FXR1	FMR1(Fragile X Mental Retardation) autosomal homolog 1
HR	Homologous recombination
HU	Hydroxyurea
IR	Ionizing radiation
MMR	Mismatch repair

MRE11	Meiotic recombination 11
NBS	Nijmegen breakage syndrome
NBS1	Nijmegen breakage syndrome 1
NER	Nucleotide excision repair
NHEJ	Non-homologous end joining
NLS	Nuclear localization signal
RAD50	Radiation sensitive 50
ROS	Reactive oxidative species
RPA	Replication protein A
SDSA	synthesis-dependent strand annealing
SLFN	Schlafen
SSB	DNA single-strand break
ssDNA	Single strand DNA
TOPBP1	DNA topoisomerase 2-binding protein 1
UV	Ultraviolet

Chapter 1

Introduction

1.1 DNA damage and replication stress

1.1.1 DNA damage

Genomic DNA, which stores genetic information, is the template for the basic processes of replication and transcription, making the maintenance of genetic stability critical for cell viability and growth. Each human cell is threatened by a variety of endogenous and exogenous stress which causes different types of DNA damage (**Figure 1.1**).

(a)Endogenous DNA damage

Endogenous DNA damage occurs spontaneously or in the physiological metabolic process of cells[1]. These include an oxidative modification of bases such as 8-oxoguanine (8-oxoG) or single-strand DNA break (SSB)[2,3], which is generated by reactive oxidative species (ROS) leaking from mitochondria. Another example is base pair mismatches caused by incorrect insertion of bases during DNA replication[4].

(b)Exogenous DNA damage

Extrinsic DNA damages are best exemplified by ultraviolet (UV)-induced pyrimidine dimers and ionizing radiation (IR)-induced DNA double-strand breaks (DSBs). Cell death can be induced by UV or IR, leading to apoptosis or necrosis depending on the context. Radiation can affect intracellular signaling, cell membranes, and transcription factors[5]. IR exposure produces SSB and DSB damages but also results in ROS including free radicals such as superoxide (O2·-). The latter effects can be through the radiolysis of

water and can be mimicked by H_2O_2 treatment [6]. Accumulation of ROS in cells is highly toxic by immediately reacting with biomolecules in cells, such as nucleic acids, proteins, and lipids. The toxicity includes proteins and lipids irreversible modificated, oxidative DNA damage, oxidative damage of some organelles, and abnormal redox homeostasis[7].

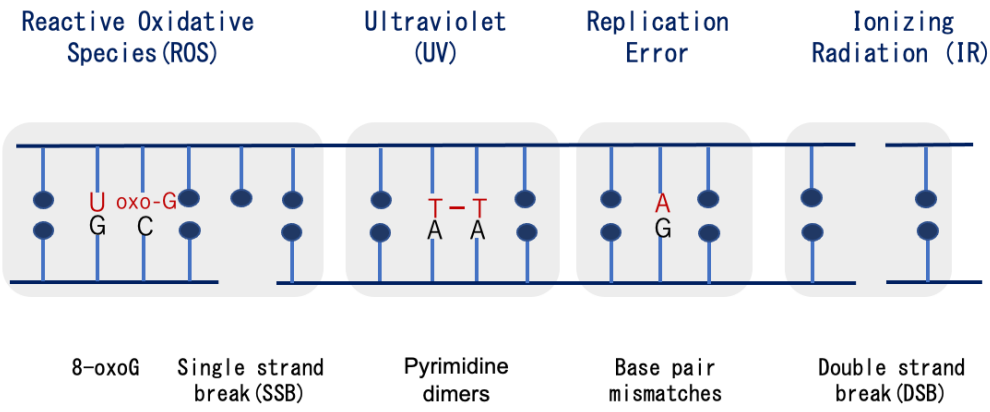

Figure 1.1 Endogenous and exogenous stress-induced DNA damage. The genomic DNA of mammalian cells is constantly challenged by endogenous stress such as reactive oxidative species (ROS) and replication errors or exogenous stress such as ultraviolet (UV) and ionizing radiation (IR).

1.1.2 Replication stress

DNA replication originate at multiple sites which referred to as origins, forming two-way replication forks. Before DNA replication, a numbers of replication initiation factors are activated for preparing the platform for replication[8]. Once replication origins fire and undergoing the replication, cells need to balance the speed, and distribution of correctly nucleotides and related replication factors to make sure replication efficiently. The unbalance of any recourse in DNA replication will lead to mutations or stalled

replication fork, which cause chromosome aberration, rearrangement, and mis-segregation. Many different sources, such as limitation of nucleotides, mis-incorporation of ribonucleotides, limitation of essential replication factors, DNA lesions, and DNA/RNA hybrids can interfere with DNA replication, and block DNA replication progression (**Figure 1.2**) [7,9-14]. This is referred to as replication stress characterized by DNA synthesis slowing down and replication forks stalling, which cause genomic instability.

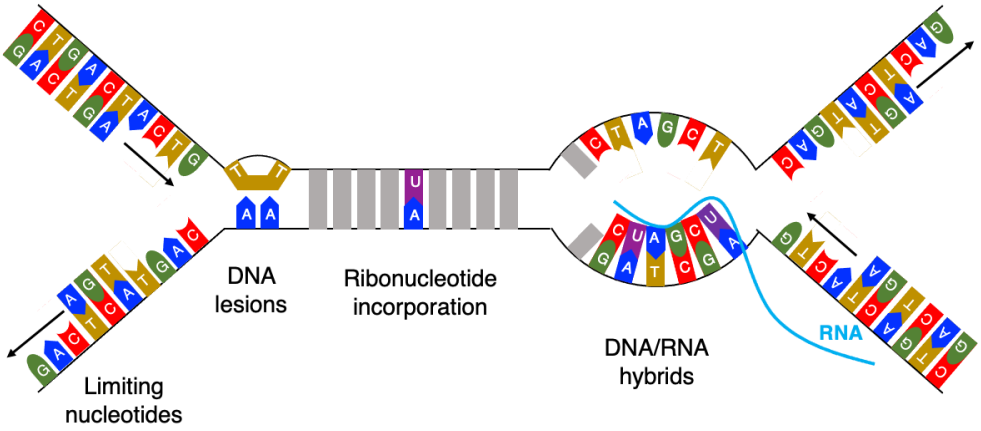

Figure 1.2 Sources lead to replication stress. There are several sources which can slow down or stalled DNA replication, including limitation of nucleotides, DNA lesions, ribonucleotide incorporation, and DNA/RNA hybrids (modified from Zeman et al 2014[15]).

1.2 Mechanisms in stress response

To counter threats posed by DNA damage, mammalian cells have evolved mechanisms termed the DNA damage responses (DDR), including DNA repair and cell cycle checkpoints[16].

1.2.1 DNA repair

Among the various DNA damages, the most threatening damage is IR-induced DNA double strands break (DSB) damage. If not repaired immediately and properly, accumulation of lesions leads to loss of genetic information, chromosomal abnormalities, cell death, and cancer. Therefore, the repair of DSB damage is extremely important for life. Mammalian cells sense DSB damage as soon as it occurs and activate the DSB repair pathway[14]. Phosphorylation of histone H2AX is one of the earliest and upstream events in DDR[17]. Genomic DNA forms nucleosomes by coiling around core histones, which are octamers consisting of histones H2A, H2B, H3, and H4, and then folds three-dimensionally into chromatin and localizes in the cell nucleus. Histone H2AX, a variant of histone H2A, is known to account for 10 to 15% of all histone H2A pools [18]. When DSB damage occurs due to IR exposure, H2AX around the DSB sites are phosphorylated[19]. Phosphorylated H2AX, termed γH2AX, plays an important role in activating DSB repair through interactions with various DDR-related factors to promote their recruitment/accumulation at DSB sites[20].

DSB damage is known to be repaired mainly by two major pathways, non-homologous end joining (NHEJ) and homologous recombination (HR) [21,22](**Figure 1.3**). In the

NHEJ repair pathway, a DNA-binding protein complex (a heterodimer composed of KU70 and KU80) first recognizes DSB and binds to the ends. DNA-dependent protein kinase catalytic subunit (DNA-PKcs) was then recruited through binding to KU70/80 complex. In many cases, DSB ends are processed by a nuclease called Artemis, and finally, DSB ends are re-ligated by DNA ligase IV (LIG4) / X-ray repair cross-complementing protein A (XRCC4) complex[23]. NHEJ repair functions throughout the cell cycle except for the M phase. It is often considered to be an inaccurate mechanism because several to dozens of bases proximal to DSB ends are excised by Artemis nucleases during the repair process[24] (**Figure 1.3**).

On the other hand, in the HR repair pathway, which is mainly operating during S to G2 phase, the DNA ends are processed in a different manner. The meiotic recombination 11 (MRE11)- radiation sensitive 50 (RAD50)- Nijmegen breakage syndrome 1 (NBS1) complex (MRN complex) is accumulated at the DSB site and forms a complex with the DNA endonuclease CtBP-interacting protein (CTIP) to produce a nick near the end of DSB. Subsequently, exonuclease 1 (EXO1) and DNA2, which have nuclease activity, cooperate with a helicase termed BLM, to control the resection of DSB ends from the 5′-terminated strand to expose a 3′-terminated single-stranded (ss)DNA tail[25]. The ssDNA 3’ends are stabilized by coating with the replication protein A (RPA) trimeric complexes (formed by RPA14, RPA32, and RPA70). With the function of breast cancer susceptibility gene 2 (BRCA2) and other factors, the RPA complex is replaced with RAD51, forming filaments in which RAD51 is polymerized on ssDNA. RAD51 then catalyzes the invasion of the nucleoprotein filament into homologous DNA, and the invading DNA strand forms base pairing with a complementary strand. Next, DNA synthesis occurs from the end of invaded strand, and anneals with a strand at the other

end of DSB. This mode of HR repair is called “synthesis-dependent strand annealing” (SDSA) pathway and mitotic cells predominantly utilize this mode[26]. In the other mode of HR repair, the broken DNA and invaded template strands form “double Holliday structure” which is then cleaved by specialized nucleases (Holliday junction resolvases) (with or without crossover) or dissolved by the BLM helicase complex (without crossover)[25,27]. Thus, HR repair is limited to occur during the S-phase to G2-phase where sister chromatids can serve as a template. HR repair is considered an accurate repair because it basically functions by “copy and paste” of nucleotide sequences (**Figure 1.3**).

The choice of whether to resect broken DNA end is a critical regulatory step that affects DSB repair pathway (NHEJ versus HR). Mis-regulation of the balance between these two key DSB repair pathways lead to genome instability that is found in many cancer types[28,29].

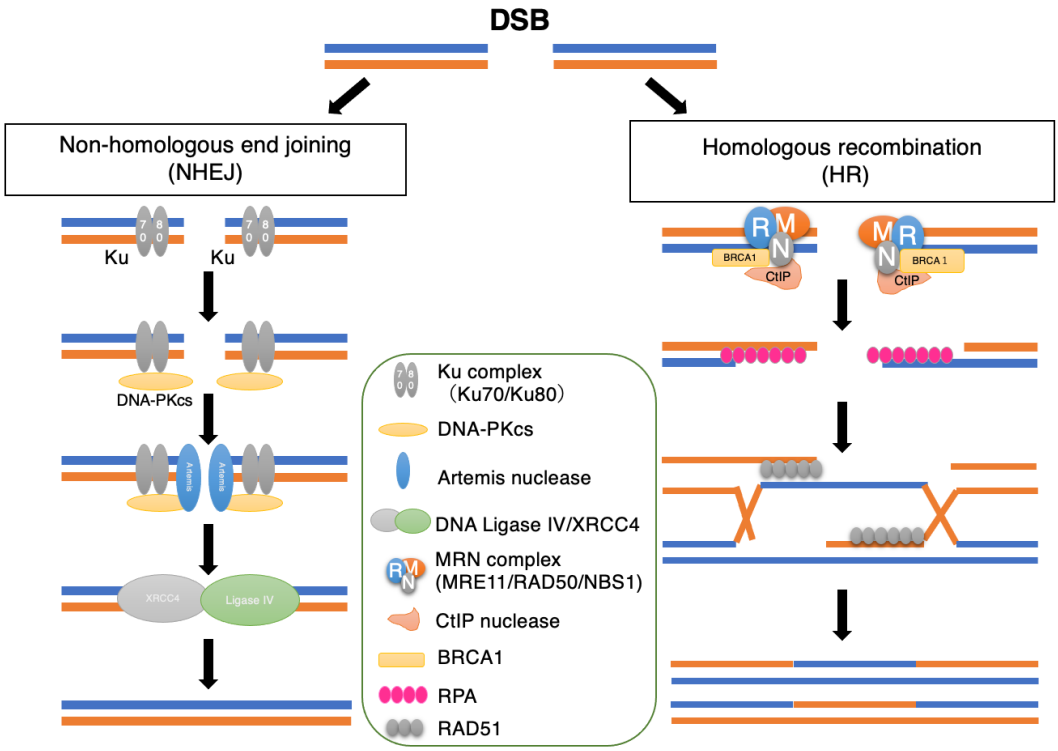

Figure 1.3 DSB repair pathway. There are two main repair mechanisms for DSB damage caused by agents such as IR: non-homologous end rejoining (NHEJ) and homologous recombination (HR). NHEJ repair directly rejoins DSB ends, whereas HR repair requires homologous sister chromatids as a template because it functions by "copy and paste" mechanisms.

1.2.2 Cell cycle checkpoint activation

To detect the occurrence of DNA damage immediately and arrest cell proliferation at a specific time to ensure DNA repair, mammalian cells utilize a mechanism termed cell cycle checkpoints[30]. Years of research have revealed that ATM (Ataxia-telangiectasia mutated) kinase is the central regulator of cell cycle checkpoints upon DSB. ATM kinase normally exists as an inactive dimer (or multimer). When DSB damage occurs, it autophosphorylates at Ser1981 and dissociates into monomers[30]. Subsequently,

monomeric ATM associate with the C-terminus of NBS1 of the MRN complex thereby accumulating at DSB sites, and exhibiting kinase activity[31]. Activated ATM kinase phosphorylates cell cycle checkpoint regulators such as p53 and CHK2 (checkpoint kinase 2) in response to DSB damage[32]. On the other hand, H_2O_2 also activates ATM in the absence of DSBs, through disulfide-cross-linking dimerization of ATM. Thus, ATM is a crucial redox-sensor for oxidative stress defense system in cells[33] (**Figure 1.4**).

When replication fork is stalled, the persisted ssDNA adjacent to the stalled newly replicated double-stranded DNA is bound by replication protein A (RPA)[25,34], which generates a signal for activation of the replication stress response. ssDNA-bound RPA serves as a signaling platform to recruit numbers of replication stress response proteins, including the protein kinase ATR kinase (ATM and Rad3-related)[35]. ATR is the central replication stress response kinase, and forms a complex with ATRIP (ATR-interacting protein). The ATR-ATRIP complex is recruited by the RPA complex on ssDNA generated by replication stress. At the same time, RAD17 complex (RAD17-RFC), RAD9-RAD1-HUS1 complex (9-1-1), and TOPBP1 (DNA topoisomerase 2-binding protein 1) are accumulated on ssDNA/dsDNA junctions generated by replication stress[36]. ATR kinase is activated by binding with the ATR-activating domain of TOPBP1 and subsequently phosphorylates downstream substrates such as CHK1 (checkpoint kinase 1), which helps the cell to survive and faithfully complete DNA replication in the face of the stress[37] (**Figure 1.4**).

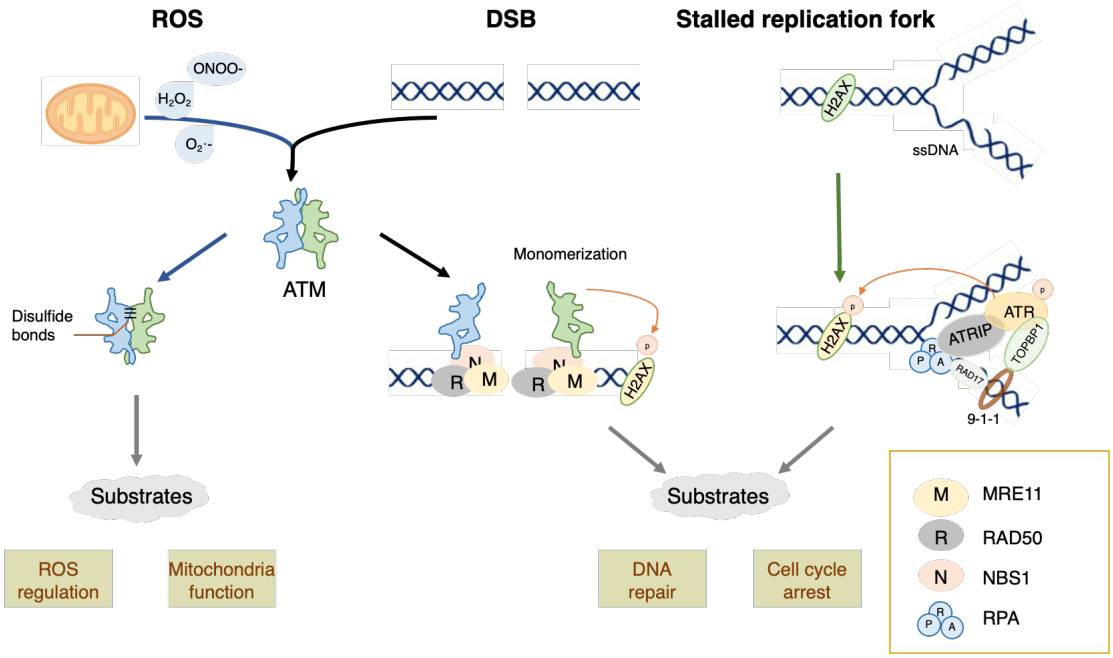

Figure 1.4 ATM, ATR activation. ATM is activated during DSB damage to regulate DNA repair and cell cycle checkpoint or cellular response to ROS. On the other hand, ATR is activated in response to replication stress.

1.2.3 Replication stress response

ATR is activated at a stalled replication fork formation and there are two key outcomes of ATR activation. One is the cell cycle arrest and another one is late origin firing suppression[38]. These events provide enough time for DNA repair and allow the cell to maintain resources to finish DNA synthesis near the stalled replication forks. ATR pathway stabilizes the stalled replication forks and the stalled replication forks can be restarted after remove the replication stress. On the other hand, restart pathways that can activate during the present of stress, as form an unrepaired DNA lesion. Replication forks stalled at DNA lesions can be rescued by the dormant origin firing[39-41]. Then, the

replication machinery can restart the replication behind the lesion and leave a “gap” on ssDNA[42,43].

Recent evidence has also demonstrated that stalled replication forks can reverse mediated by fork remodeling enzymes (e.g., ZRANB3, HLTF, SMARCAL1) and RAD51, unwinding the double strand DNA and result in the newly replicated strands with a “chicken foot” structure. Reversed fork structures form more often when the checkpoint pathway is inactivated[44,45], and stalled forks are degraded by nuclease such as DNA2 and MRE11 in the absence of ATR signaling[46-48]. This degradation is prevented by HR-independent functions of DNA damage response proteins, such as RAD51, BRCA1, BRCA2, FANCD2 and RPA [47][48], resulting in the promotion of stalled fork recovery[49]

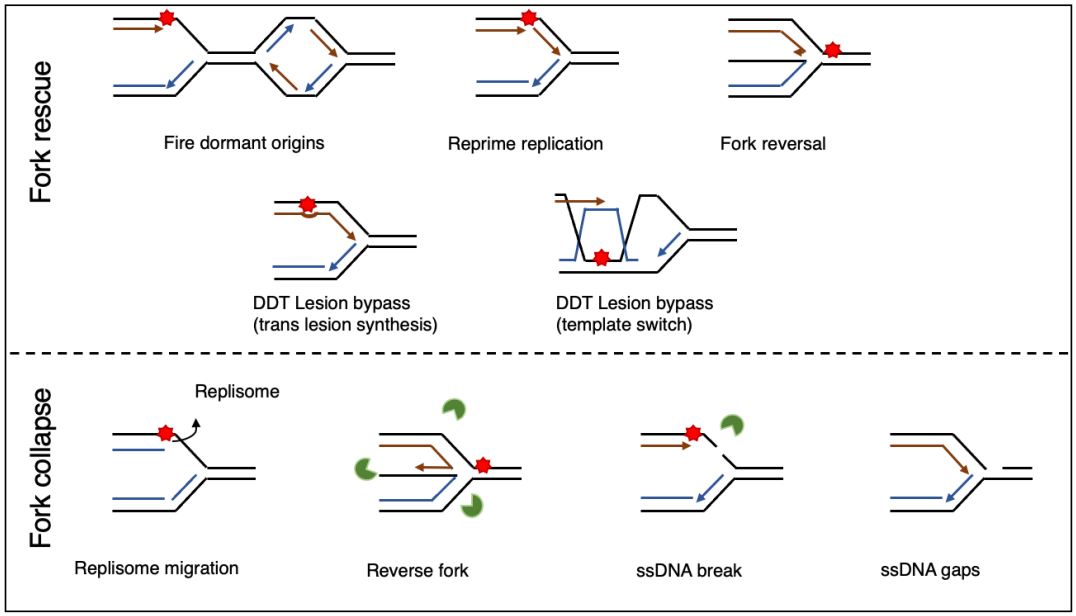

Figure 1.5 Mechanisms of rescue and collapse stalled replication fork. (Upper) Mechanisms of the fork rescue. Replication fork was stalled by DNA lesion (shown as red star) can restart replication with formation of fire dormant origins, repriming replication, reversal stalled fork, or

activating the DNA damage responses. **(Below)** Mechanisms of fork collapse. The mechanism that includes dissociation of replisome components, nuclease degradation of a reversed fork, or ssDNA gaps are shown (modified from Zeman et al. 2014[15]).

1.3 Human Diseases and the cellular response to genotoxic stress

Genotoxic stress such as DNA damage and replication stress can lead to mutations, genomic instability, loss of stem cells, aging and cancer. In particular, several diseases are associated with defects in DNA damage and replication stress response signaling. The *ATM* gene encoding ATM kinase was identified in 1995 as the causative gene for ataxia-telangiectasia (A-T), a radiation-sensitive genetic disorder[32]. Patients with A-T exhibit radiation-resistant DNA synthesis (RDS), which is a cytological signature resulting from radiation-induced cell cycle checkpoint dysfunction caused by ATM gene defects[50,51].

As ATR activation is a key initiating event in the replication stress response, human with mutant of either ATR alleles that reduce protein expression, or with mutations in ATRIP, a binding partner of ATR, lead to Seckel syndrome, which is characterized by developmental delay, microcephaly, and mental retardation[52-54]. Similarly, loss of NBS1 and MRE11, which activates ATM upon DSB, has been associated with developmental disorders NBS and ATLD, respectively[55,56]. ATLD show similar clinical features of progressive cerebellar ataxia like A-T[56]. Patients lacking this NBS1 or MRE11 have a combination of cellular features associated with loss of DNA damage stress signaling and defects in DSB repair. The defective cellular stress response also leads to the accumulation of unrepaired DNA damage, leading to genomic instability and

mitochondrial dysfunction, causing progressive loss of neuronal cells, contributing to neurodegenerative disorders [58-60] (**Table 1**).

Probably the most common human disease associated with DNA damage and replication stress is cancer. Genome instability is a hallmark of cancer[57]. For example, genomic instability in lymphoid tumors often display chromosomal translocations in which proto-oncogene loci are fused to those of an antigen receptor[58,59], apparently through aberrant antigen receptor rearrangements. Furthermore, the mismatch repair deficiency (in Lynch syndrome) causes microsatellite instability (MIN) in colorectal and endometrial cancers[60]. In addition, chromosomal instability (CIN) is observed in most sporadic solid tumors[61].

Table 1 Human Diseases Related with Cellular Response Defects

Defect gene	Syndrome	Characteristics
ATM	Ataxia telangiectasia(AT)	Cerebellar ataxia, telangiectases, immune defects, predisposition to malignancy
NBS1	Nijmegen breakage syndrome (NBS)	Microcephaly, growth retardation, mental retardation, immunodeficiency, cancer predisposition
MRE11	Ataxia telangiectasia-like disorder (ATLD)	Mild A-T like features, possibly cancer predisposed
ATR, SCKL2, SCKL3	Seckel syndrome	Marked microcephaly, primordial dwarfism, dysmorphic facial features and mental retardation, possibly AML
RAD50	NBS-like syndrome	NBS-like phenotype
Increased oxidative stress and damage	Alzheimer's disease	Progressive neurodegeneration leading to dementia, memory loss and cognitive decline
Senataxin	Amyotrophic lateral sclerosis 4	Childhood- or adolescent-onset degeneration of motor control

However, defects in the function of DNA damage response or replication stress response not only promote tumor development but also make cancer cells more vulnerable to DNA-damage agents. This is the basis for cancer treatments which utilize DNA damaging agents. Even though the recent development of immune checkpoints

inhibitor drugs (anti-CTLA4 or anti-PD-1/PD-L1 antibodies)[62], most widely used cancer drugs are still DNA-damaging agents like cisplatin[63,64]. These chemotherapeutic drugs often kill cancer cells by inducing replication stress. Therefore, it is of foremost importance to understand the mechanisms of replication stress in cancer cells. Recent studies indicate that expression of SLFN11 gene in cancer cells accelerates chemotherapeutic response in cell lines and patients undergoing chemotherapy[65-68]. It is also reported that SLFN11 can affect replication stress response. However, mechanistically how SLFN11 can affect cell fate decisions following DNA damage remains unclear. In particular, how two main functional domains in SLFN11 protein, N-terminal ribonuclease (RNase) domain and C-terminal helicase domain, contribute to DNA damage sensitivity is controversial, and needs to be clarified.

1.4. Aim of the study

Increasing the understanding of DNA damage and replication response not only deepens our knowledge of how the disease develops but also contributes to developing drugs exhibiting therapeutic efficacy towards neurodegeneration disorders and cancer cells. To gain novel insights regarding these disorders and related mechanisms, I investigated the function of DNA damage and replication stress response related protein MRE11 and its novel binding protein FXR1 in response to oxidative stress in chapter 2. In chapter 3, the function of N-terminal RNase domain of SLFN11 during replication stress was investigated.

Chapter 2

FXR1 is a novel MRE11-binding partner and participates in oxidative stress responses

2.1 Introduction

Radiation-hypersensitive disorders have been useful to identify the underlying mechanisms of DNA damage responses following IR. One of the best known of these is ataxia-telangiectasia (AT). AT is an autosomal recessive disorder primarily characterized by radiosensitivity, progressive cerebellar ataxia, cerebellar degeneration, telangiectasia, immunodeficiency, and cancer susceptibility. Cells derived from AT patients commonly show radiation hypersensitivity, radio-resistant DNA synthesis (RDS), and chromosome aberrations[69,70]. The gene responsible for AT is *ATM*, whose product ATM is a protein kinase[69,70].

Similarly to AT, genetic defects in Nijmegen breakage syndrome (NBS), or ataxia-telangiectasia-like disorder (ATLD) also show cellular phenotype radiation hypersensitive[70], which responsible genes are *NBS1* and *MRE11* respectively. As mentioned before, MRE11/RAD50/NBS1 (MRN) binds to ATM monomer and promotes its recruitment to DSB damage sites. ATM then phosphorylates several DDR factors, such as p53, Chk2, and SMC1, in turn activating cell cycle checkpoints[71]. The typical RDS cellular phenotype in AT is due to a defect of the cell cycle checkpoint in the S phase. Research on these radiation-hypersensitive disorders suggests that defective function in DDR underlying cause of their cellular phenotype[72].

Although AT, NBS, and ATLD share a similar cellular phenotype, some of their clinical manifestations are distinct, particularly the neurodegeneration phenotypes. AT and ATLD patients show progressive cerebellar ataxia, whereas almost all NBS patients show microcephaly[70]. However, the genes involved in cell cycle checkpoints and DSB repair are not accountable for the neurodegeneration phenotypes. Ataxia–oculomotor

apraxia (AOA) is a phenotype related to cerebellar ataxia and is also found in AOA1, AOA2, and AOA3 along with AT and ATLD[73]. Aprataxin, the product of the gene causing AOA1, participates in DNA single-strand break repair[74,75] while senataxin, the gene product responsible for AOA2, is crucial to resolve DNA–RNA hybrid formation (R-loop) in transcript-related DNA damage[76]. In AOA3, cytochrome *b* is mutated, and the patient-derived cells show abnormal mitochondrial dynamics[77,78]. Neural stem cells are known to be sensitive to oxidative stress, and neural cells from *ATM*-deficient mice show decreased viability. However, radical scavenger treatment recovers the viability of *ATM*-deficient cells[70,79,80], suggesting that ATM function is pivotal to resisting oxidative stress *in vitro* and might be indispensable for the viability of neural cells in the cerebellum. Indeed, although ATM kinase activation is dependent on DSB damage generation, it can also occur following oxidative stress[70]. Guo et al. reported that oxidative stress by H_2O_2 treatment causes ATM activation *in vitro* and *in vivo*, likely due to the formation of disulfide bonds causing a conformational change of the ATM dimers[33]. Consistent with this, it has been reported that AOA3-patient cells showed excessive accumulation of reactive oxygen species (ROS), particularly the mitochondria-related ROS superoxide, which perturbed ATM-dependent phosphorylation[77,78]. It is also showed that induction of superoxide by pyocyanin treatment suppressed ATM-dependent phosphorylation. Collectively, evidence suggests that the oxidative stress caused by ATM function defects might lead to neurodegeneration phenotypes in AOA3 cells.

As ATLD and AT patients show similar neurodegeneration phenotypes, I hypothesized that *MRE11*-deficient ATLD cells may harbor ATM function defects and MRE11 may be important for ATM activation upon oxidative stress. I found that MRE11 participates

in ATM activation in response to H_2O_2 or pyocyanin-induced oxidative stress. FXR1 was identified as a novel cytoplasmic MRE11-binding partner and showed that it also participates in the oxidative stress response. Finally, the role of MRE11 and FXR1 in cellular response against oxidative stress was discussed.

2.2 Materials and methods

2.2.1 Cell culture

HeLa, U2OS, hTERT immortalized human fibroblasts (48BR), SV40 virus-transformed human fibroblasts (MRC5SV), SV40 virus-transformed ATLD patient-derived fibroblasts (ATLD2SV and HMfibroSV) and A-T patient-derived Fibroblasts (AT5BIVA) were cultured in Dulbecco's Modified Eagle Medium (DMEM; Gibco) supplemented with 10% fetal bovine serum (FBS; Invitrogen) and antibiotics. Mutated MRE11 in ATLD2SV has a nonsense mutation and expresses C-terminal-truncated MRE11 protein, and mutated MRE11 in HMfibroSV has a missense mutation, in which the MRE11 protein is unstable.

2.2.2 Generation of GFP-FXR1-expressing cells

Human FXR1 (FBL, NM_005087.4) and MRE11 (MRE11, NM_005591) were amplified from a human fetal cDNA library (Clontech) by PCR with Pyrobest DNA polymerase (TAKARA). Then, FXR1 cDNA was inserted into pEGFP-C1 (Clontech) vectors, and MRE11 cDNA was inserted into pCMV-Tag2B-FLAG (Promega) vectors; the insertions were confirmed by DNA sequencing.

2.2.3 siRNA knockdown experiment

Sub-confluent cells were plated on culture dishes for 24 h and then transfected with siRNAs targeting MRE11 (B-Bridge International Inc.), NBS1 (B-Bridge International Inc.), RAD50 (B-Bridge International Inc.), and FXR1 (Qiagen Co.), or with negative control siRNA (B-Bridge International Inc.) using Lipofectamine RNAiMax (Invitrogen Life Technology). Cells were re-plated and used for each experiment after 24 h of siRNA treatment.

2.2.4 Drug treatment

Pyocyanin is a substance secreted outside the body of *Pseudomonas aeruginosa* and inhibits mitochondrial electron transfer thereby inducing mitochondrial oxidative stress. For pyocyanin treatment, pyocyanin (WAKO) was made into a 10 mM stock solution in DMSO (Sigma-Aldrich). An amount required for the experiment (described in the legend of the figure) was added and treated for the indicated time.

Cells were exposed to 100 μM hydrogen peroxide (H_2O_2) (WAKO) for indicated time to induce oxidative stress.

2.2.5 Western blot analysis

After IR or drug treatment, cells were harvested and washed with PBS twice. The cells were lysed with RIPA buffer (20 mM Tris-HCl [pH 8.0], 2 mM EDTA, 150 mM NaCl, 0.1% SDS, 1% NP-40) containing protease inhibitors and phosphatase inhibitors and incubated on ice for 10 min. After centrifugation, the lysate was boiled at 95°C for 5 min. After quantifying the protein extract using a protein assay staining solution (Bio-Rad), 50

μg of the protein extract was subjected to sodium dodecyl sulfate-polyacrylamide gel electrophoresis (SDS-PAGE) for about 2 h. Electrophoresed proteins were transferred to an Immobilon-P membrane (Millipore) at 15V (constant voltage condition) at room temperature for 0.5 h. The transferred membrane was gently shaken in a blocking solution (5% skim milk/TBST) at room temperature for 1 h. The membrane was washed gently with TBST. Then, the membrane was reacted with primary antibody, diluted by skim milk/TBST at 4 ℃ overnight. After the reaction of the primary antibody, the membrane was washed with TBST for 10 min three times and then reacted with HRP (horseradish peroxidase)-labeled anti-rabbit IgG or anti-mouse IgG secondary antibody (GE Healthcare) diluted by 1% BSA/TBS-T for 1 h at room temperature. After the reaction of the secondary antibody, the membrane was washed with TBST for10 min 3 times. The membrane was reacted with ECL plus chemiluminescence system (GE Healthcare) for 5 min at room temperature, then target proteins were visualized by exposure to X-ray film.

2.2.6 Immunoprecipitation analysis

After IR or drug treatment, cells were harvested and suspended in IP buffer (10 mM Tris/HCl [pH7.8], 1% NP-40, 150 mM NaCl, 1 mM EDTA) containing protease inhibitors and phosphatase inhibitors, and placed on ice. After centrifuging (4°C, 15,000 rpm, 10 min), the supernatant was collected as a protein extract. After protein quantification, a fixed amount of the protein extract was placed in a microtube, an anti-MRE11 rabbit polyclonal antibody was added, and the mixture was incubated on ice for 1 h. Subsequently, Protein-A Sepharose (GE Healthcare) was added and reacted overnight at 4°C with rotation. The next day, centrifugation (4°C, 10,000 rpm, 1 min) was

performed to separate co-immunoprecipitated protein complexes. The target protein contained in the separated complex was detected by Western blotting as shown in 2.2.5.

2.2.7 Immunofluorescence staining

The day before the experiment, 300 μl of a 2×10^5 cells/ml cell suspension was seeded on a MAS-coated glass slide (MATSUNAMI) placed in a 100 mm culture dish, dry for 10 min in a CO_2 incubator, then 10 ml of culture medium was added and cultured overnight. After damage treatment, the tissue was immersed in cold 100% methanol (Nacalai Tesque) and incubated at 4°C for 20 min for fixation. After washing with PBS, cells were permeabilized with 0.5% Triton X-100/PBS at 4°C for 10 min, then washed again with PBS, and blocked with 5% BSA/PBS for 20 min at room temperature. Subsequently, a primary antibody solution diluted to an appropriate concentration with PBS was dropped onto the sliding glass, covered with a cover glass, and reacted at room temperature for about 1 h. After washing the sliding glass with PBS, slides were incubated with secondary Alexa594-labeled mouse IgG antibody and Alexa488-labeled rabbit IgG antibody (Molecular Probes) solution diluted by 1.5% BSA/PBS for 1 h in the dark. After washing the sliding glass with PBS, DAPI (Vector Laboratories, Inc.), a nucleic acid staining reagent, was added dropwise, covered with a cover glass, sealed with nail polish, and observed under a fluorescence microscope (Leica).

2.2.8 ATM kinase activity assay

After treatment with γ-irradiation or H_2O_2, cells were harvested and added TGN buffer (50 mM tris [pH 7.5], 50 mM glycerophosphate, 150 mM NaCl, 10% glycerol, 1% Tween

20, 1 mM NaF, 1 mM $NaVO_4$, 1 mM phenylmethyl sulfonyl fluoride, 2 μg/mg pepstatin A, 5 μg/ml leupeptin, 10 μg/ml aprotinin, and 1 mM dithiothreitol), followed by centrifugation (15,000 rpm) to extract the whole-cell protein. 3 mg of cell extract was added with a rabbit polyclonal antibody to anti-ATM, followed by immunoprecipitation of ATM complexes with Protein-A Sepharose (GE Healthcare). ATM immunoprecipitants were washed twice with TGN buffer and once with 100 mM Tris (pH 7.5) containing 0.5 M LiCl, followed by kinase buffer (10 mM HEPES [pH 7.5], 50 mM glycerophosphate, 50 mM NaCl, 10 mM $MgCl_2$, 10 mM $MnCl_2$, 5 μM ATP, and 1 mM DTT). The cells were suspended in 30 μl of kinase buffer containing 10 μCi (γ-32P) ATP and 1 μg GST-p53 and reacted at 30°C for 30 min. The phosphorylation of p53 (ATM substrate) by immunoprecipitated ATM was estimated by western blot analysis using anti-phospho-p53 (S15) antibody (Cell Signaling) and mouse monoclonal anti-GST (GE Healthcare).

2.2.9 HR repair activity analysis

HR repair activity was carried out using HeLa cells transfected with a Direct Repeat (DR)-GFP reporter gene. To measure HR repair activity, 50 μg of I-SceI restriction enzyme expression vector (pCBASce) was introduced into 1×10^6 HeLa-DRGFP cells by electroporation (GenePulser; Bio-Rad) and incubated for 24 h to generate DSBs. The next day, the cells were collected and washed with PBS, replaced with a new medium, and cultured for 48 h. The percentage of GFP-positive cells repaired by HR was measured with a FACSCalibur™ flow cytometer (Becton Dickinson).

2.2.10 Mass spectrometry analysis

293E cells were transfected with the generated pCMV-Tag2B-FLAG MRE11 plasmids using FugeneHD (Promega) and harvested after 2 days. Cytoplasmic and nuclear fractions were extracted from the harvested cells and were used for immunoprecipitation with anti- FLAG antibody (Sigma-Aldrich). The candidate MRE11-binding proteins in immunoprecipitants were identified by an HPLC-mass spectrometer (AB SCIEX Co.).

2.2.11 Propidium iodide staining to detect apoptosis

Cells were treated with camptothecin (CPT) and then harvested at the indicated time, followed by fixed with 70% ethanol and then incubated at −20℃ overnight. Fixed cells were treated with RNase (5 mg/ml) and stained with propidium iodide (PI; 50 μg/ml). The apoptotic fractions (sub-G1) were quantified using a flow cytometer (Becton Dickinson).

2.2.12 Antibodies

The primary antibodies used in Western blot, immunoprecipitation, immunofluorescent staining, and ATM kinase activity assay were shown in Table 2.1.

Table 2.1 Anti-bodies list

Antibodies	Catalog	Source
Phosphor-ATM(S1981)	Ab81292	Abcam
ATM	sc-23992	Santa Cruz Biotechnology
RPA70	NA-18	Merk Millipore
RPA32	NA-19 L6	Merk Millipore
Phosoho-CHK1(S317)	2344	Cell Signaling Technology
FXR1	A300-892A	Bethyl Laboratories
Phospho-CHK2(T68)	2661	Cell Signaling Technology
H2B	07-371	Merk Millipore
KAP1	64422	Gentex
Phospho-KAP1(S824)	A300-767A	Bethyl Laboratories
Phospho-p38MAPK	4511	Cell Signaling Technology
MRE11	GTX70212	Gentex
MRE11	NB100-142	Novus
RAD50	GTX70282	Gentex
RAD50	A53169	Sigma-Aldrich
NBS1	NB100-143	Novus
NBS1	GXT70222	Gentex
Phospho-p53(S15)	9286	Cell Signaling Technology
p53	Sc126	Santa Cruz Biotechnology
Phospho-RAD17(S645)	6981	Cell Signaling Technology
Phospho-RPA32	A300-246A	Bethyl Laboratories
Phospho-SMC1	A300-050A	Bethyl Laboratories
SMC1	A300-055A	Bethyl Laboratories
RAD51	70-001	Biocademia
βactin	A53169	Sigma-Aldrich
γH2AX	05-636	Merk Millipore
GST	27-4577-01	GE Healthcare
TOMO20	11082-1-AP	ProteinTech
H2B	07-371	Merk Millipore

2.3 Results

2.3.1 MRE11 participates in ATM activation following oxidative stress

To clarify the interplay of ATM and MRE11 in oxidative stress responses, I firstly investigated ATM-dependent phosphorylation following H_2O_2 treatment in MRE11-defective ATLD patient fibroblasts **(Figure 2.1)**. H_2O_2 treatment induced auto-phosphorylation of ATM in normal MRC5SV cells and increased the phosphorylation of ATM substrates SMC1, Chk2, and p53. However, γ -H2AX, the marker of DSBs, did not increase remarkably **(Figure 2.1 AB)**, suggesting that this treatment did not cause the generation of DSB. Intriguingly, in *MRE11* depleted ATLD-patient cells (HMfibroSV and ATLD2SV cells), ATM auto-phosphorylation and phosphorylation of ATM substrates (SMC1, Chk2, and p53) did not increase significantly after the H_2O_2 treatment **(Figure 2.1 AB)**. siMRE11 knockdown U2OS cells also showed decreased ATM auto-phosphorylation and SMC1 phosphorylation similarly to ATLD-patient cells **(Figure 2.1 C)**.

To elucidate the functional role of MRE11 in ATM activation upon oxidative stress, I tested ATM activity *in vitro* by analyzing the phosphorylation of its substrate p53 **(Figure 2.1 D)**. Anti-ATM immunoprecipitants from C2ABR cells after irradiation or H_2O_2 treatment showed full ATM activity, while immunoprecipitants from MRE11-deficient ATLD2ABR cells did not, suggesting that MRE11 is essential for ATM activation in response to oxidative stress.

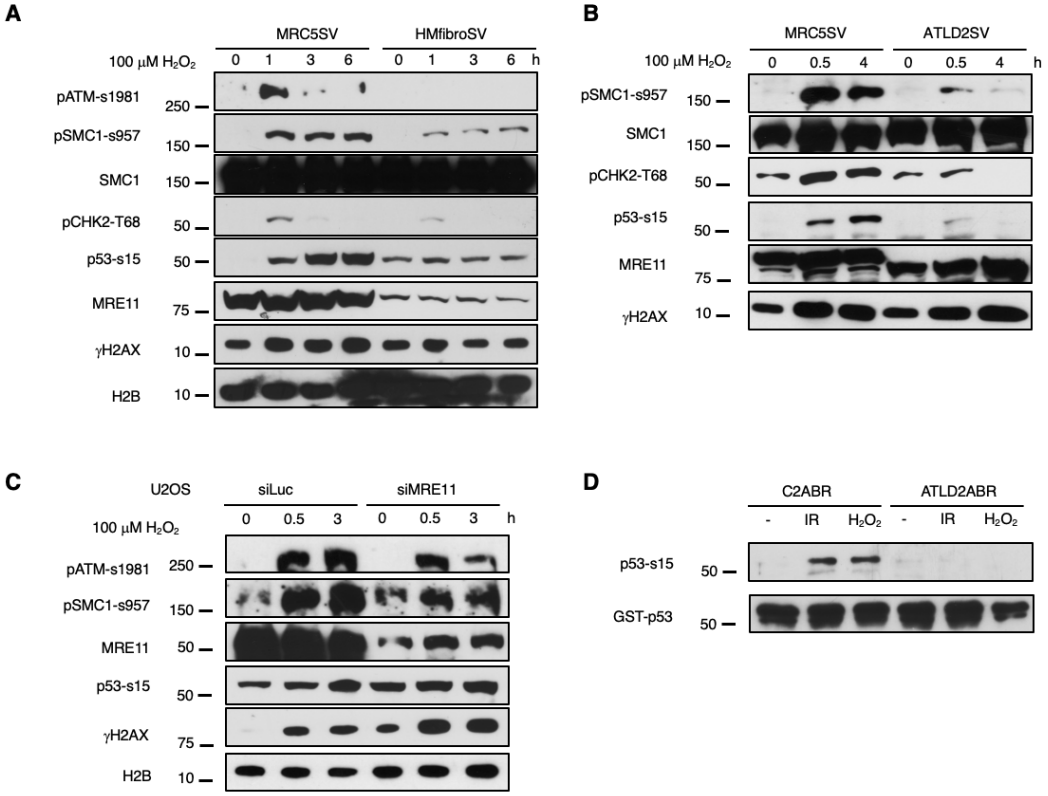

Figure 2.1 MRE11 participates in ATM activation following oxidative stress. (A) MRC5SV and *MRE11*-deficient HMfibroSV (HM) cells were treated with 100 mM H_2O_2 for indicated times and analyzed using the indicated antibodies. **(B)** MRC5SV and *MRE11*-deficient ATLD2SV(ATLD2) cells were treated with 100 mM H_2O_2 for the indicated time, and Western blotting was performed using the antibodies shown in the figure. **(C)** U2OS cells were transfected with siRNA targeting MRE11. After 48 h, these cells were treated with 100 mM H_2O_2 for the indicated times and analyzed using the indicated antibodies. **(D)** Normal C2ABR or *MRE1*1-deficient ATLD2ABR lymphoblastoid cells were treated with 10 Gy γ-irradiation and 100 mM H_2O_2, cells were harvested after 1 h, and ATM immunization was performed using an anti-ATM antibody. Conjugates were generated and subjected to kinase activity assays. Phosphorylation of the substrate p53 was detected by Western blotting using an anti-phospho-p53 antibody. Expression of the substrate p53 was detected by Western blotting using an anti-GST antibody.

Next, I examined ATM-dependent phosphorylation by H_2O_2 treatment using NBS patient cells that lack the *NBS1*. I found that ATM-related phosphorylation increased in NBS1-defective patient cells after H_2O_2 treatment, but not in A-T patient cells that lack *ATM* **(Figure 2.2 A)**. In addition, knockdown of RAD50 did not perturb ATM-dependent phosphorylation suggesting that MRN complex components NBS1 and RAD50 are not involved in the activation of ATM in response to oxidative stress **(Figure 2.2 B)**.

Mitochondria generate and accumulate superoxide, and ATM is known to localize in mitochondria to function in oxidative stress response [81]. Hence, whether MRE11 is localized to mitochondria was next investigated. I prepared the mitochondrial fraction using a Mitochondria Isolation Kit (Thermo Scientific) and performed western blot assay. MRE11 was detected in the mitochondrial fraction in normal MRC5SV and *ATM*-deficient AT cells. **(Figure 2.2 C)**. Taken together, MRE11 partly localizes to the mitochondria, independently of ATM, and functions in ATM activation upon oxidative stress.

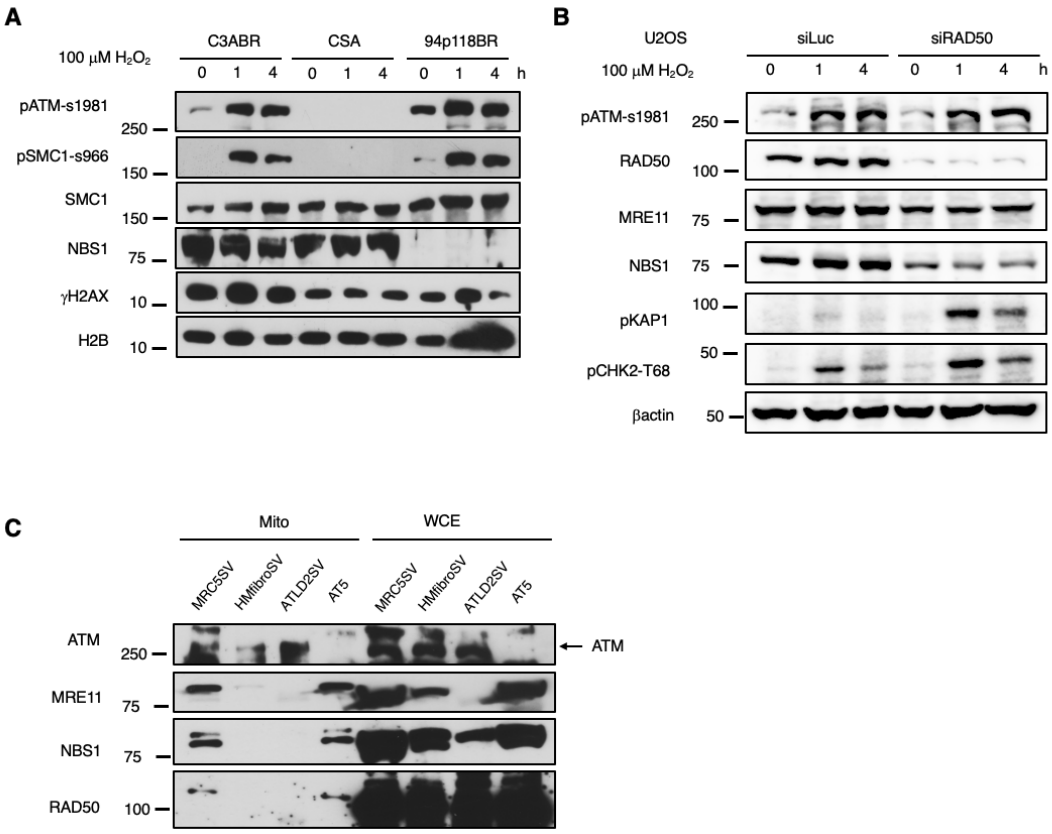

Figure 2.2 NBS1 and RAD50 are dispensable for ATM activation in response to oxidative stress. (A) Normal (C3ABR), AT (CSA), or NBS (94p118BR) lymphoblastoid cells were treated with H_2O_2 (100 μM) for indicated time and analyzed by indicated antibodies. **(B)** U2OS cells were transfected with siRNA targeting RAD50 for 48 h, then cells were treated with H_2O_2 (100 μM) for the indicated time and analyzed by indicated antibodies. **(C)** Mitochondria fractions were prepared from normal (MRC5SV), ATLD, or AT (AT5) cells using Mitochondria Isolation Kit (Thermo Scientific), and western blot analysis was performed using indicates antibodies. Mito: mitochondria; WCE: whole cell extracts.

2.3.2 FXR1 is a novel MRE11-binding partner protein

MRE11 functions in DDRs such as HR repair and ATM-dependent cell cycle checkpoints as a component of the MRN complex[22,82], but NBS1 was dispensable for ATM activation following oxidative stress **(Figure 2.2 A)**. Hence, I speculated that MRE11 may form a complex with another protein for oxidative stress responses and I tried to identify novel binding partners for MRE11 using mass spectrometry. To enrich for MRE11-containing complexes, I performed immunoprecipitation from cytoplasmic and nuclear fractions of 293E cells, transfected with either wild-type MRE11 (WT), or a mutated MRE11 (329 T) that was expressed in the ATLD patient cell line (HMfibroSV)[83]. Mass spectrometry analysis identified more than 30 candidate MRE11-binding proteins from the cytoplasmic or nuclear fractions **(Figure 2.3 A)**. As ROS are mainly generated from mitochondria in the cytoplasm, I focused on a candidate (of about 60 kDa) from the cytoplasmic fraction **(Figure 2.3 B)**. The identified protein is FXR1, whose role in the cellular responses against ROS almost unknown.

A

<Identified candidates>
- DNA replication-related; 5 genes
- Oxidative stress-related; 6 genes
- RNA-binding, RNA metabolism-related; 13 genes
- Others; 10 genes

B

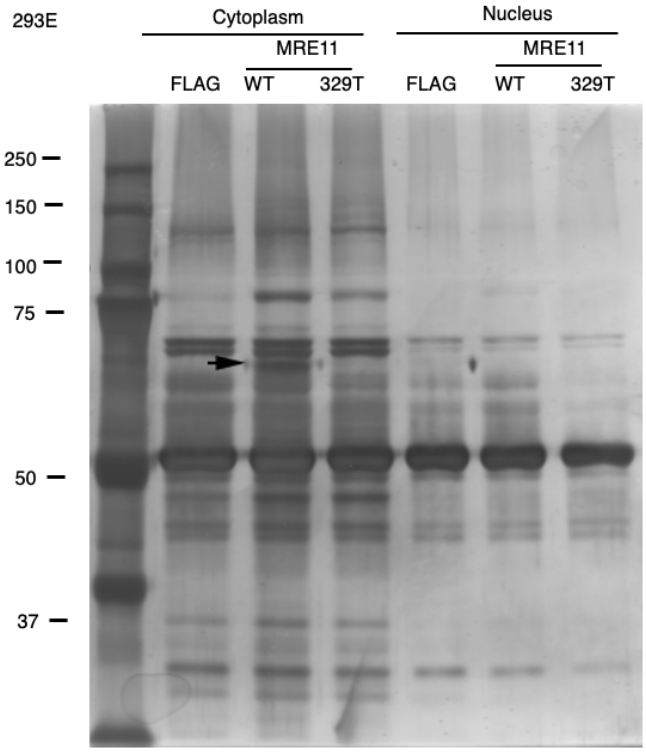

Figure 2.3 FXR1 is a novel MRE11-binding protein. (A) The list of candidates of MRE11-binding proteins with MASS spectrometry analysis. **(B)** The cytoplasmic and nuclear extracts from 293E cells expressing FLAG-tagged wild-type or a A329T mutant MRE11(expressed in MRE11-deficient ATLD patient) were collected, the MRE11-binding candidate proteins were immunoprecipitated using anti-FLAG antibodies and electrophoresis. Then, the gel was stained, cut, and digested with trypsin. The MRE11-bindig candidates were identified with MASS spectrometry. Arrow; FXR1 was identified from this band.

I next verified the interaction between FXR1 and MRE11 with immunoprecipitation and western blot analysis. Anti-MRE11 antibody precipitated FXR1 as well as RAD50, a component of the MRN complex, independently on irradiation **(Figure 2.4 A)**. The anti-NBS1 antibody also precipitated FXR1 **(Figure 2.4 B; upper panel)**. However, the interaction between MRE11 and FXR1 was also observed in NBS1- lacking patient cells and seemed higher than in normal MRC5SV cells **(Figure 2.4 B; lower panel)**, suggesting that NBS1 might be dispensable for this interaction.

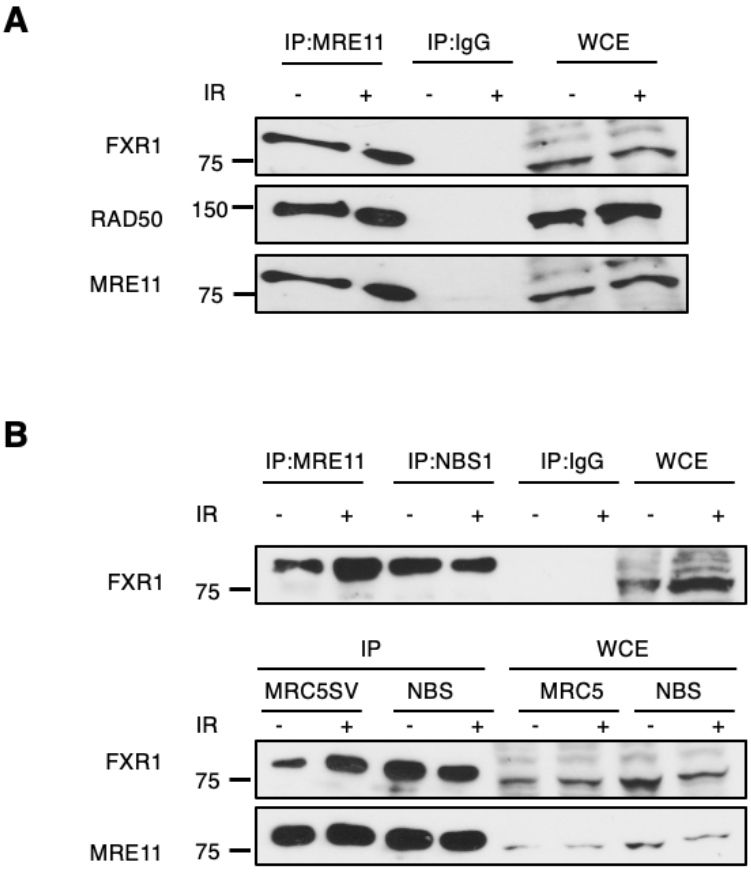

Figure 2.4 FXR1 co-immunoprecipitated MRE11(A) Extracts from C3ABR, or C3ABR **(B: upper panel)** MRC5SV and NBS1-defective NBS cells **(B: lower panel)** treated with or without 10 Gy of IR were immunoprecipitated with anti-MRE11 antibody (Novus), anti-NBS1 antibody (Novus) or anti-IgG, and then the immuno-complexes were detected by western blot analysis using the indicated antibodies. WCE = Whole cell extract.

I next examined the localization of FXR1 with immunofluorescence. FXR1 localized in the cytoplasm with or without irradiation in U2OS cells **(Figure 2.5 A)**. Furthermore, FXR1 localization didn't change following H_2O_2 or pyocyanin-induced oxidative stress **(Figure 2.5 A)**. Since NBS1 possesses a nuclear localization signal (NLS), MRE11 localizes to the nucleus upon the formation of the MRN complex with NBS1[84]. Consistent with this, MRE11 localized in the nucleus in U2OS cells, while NBS1-deficient patient NBS cells showed localization of most MRE11 in the cytoplasm, as well as FXR1, no matter whether treated with or without irradiation **(Figure 2.5 B)**. Moreover, oxidative stress treatment with H_2O_2 or pyocyanin did not influence the cytoplasmic localization of FXR1 in NBS cells **(Figure 2.5 B)**. These findings suggested that FXR1 localizes in the cytoplasm independent of NBS1. In addition, western blot analysis combination with mitochondrial fraction confirmed the successful purification with the antibody against the mitochondrial marker TOMO20. Both MRE11and FXR1 were detected in the mitochondria fraction **(Figure 2.5 C)**. These findings suggested that FXR1 and MRE11 localize in the mitochondria. However, as anti-NBS1 antibody co-precipitated FXR1 with MRE11 **(Figure 2.4 B upper panel)** and as a small portion of NBS1 is known to distribute into the cytoplasm in human cells, NBS1 may partially participate in the formation of MRE11/FXR1 complex.

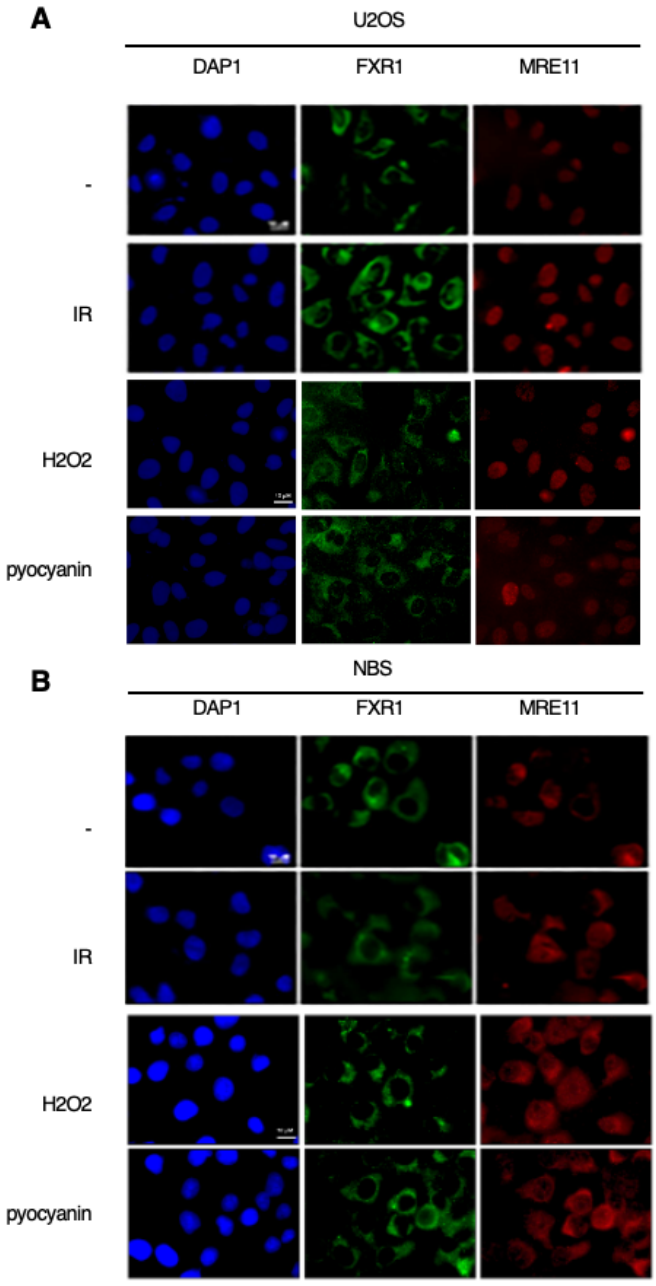
A
U2OS
DAP1
FXR1
MRE11
-
IR
H2O2
pyocyanin
B
NBS
DAP1
FXR1
MRE11
-
IR
H2O2
pyocyanin

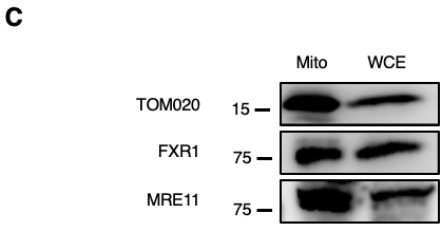

Figure 2.5 Cytoplasmic distribution of FXR1. U2OS cells **(A)** or NBS cells **(B)** were irradiated with IR (5 Gy) H_2O_2 (100 μM) or pyocyanin (50 μM). After 0.5 h, the cells were fixed and immunostaining was performed using anti-FXR1 (Bethyl) and anti-MRE11 antibody (GeneTex). **(C)**Mitochondria fractions were prepared from normal (MRC5SV) cells using Mitochondria Isolation Kit (Thermo Scientific), and western blot analysis was performed using indicates antibodies. Mito: mitochondria; WCE: whole cell extracts.

2.3.3 FXR1 may partially participate in HR repair but not in ATM activation

As MRE11 is crucial for HR repair and ATM activation, I decided to investigate the role of FXR1 in these DDRs. I verified the efficiency of FXR1 knockdown in HeLa **(Figure 2.6 A)** and U2OS cells **(Figure 2.6B)**. FXR1 protein expression in FXR1 knockdown U2OS cells and HeLa cells was markedly reduced but did not affect the expression of MRE11 and RAD50. FXR1 knockdown HeLa cells showed auto-phosphorylation of ATM and ATM-dependent phosphorylation of KAP1 and γH2AX after irradiation **(Figure 2.6)**. These findings suggest that FXR1 is dispensable for ATM-dependent phosphorylation.

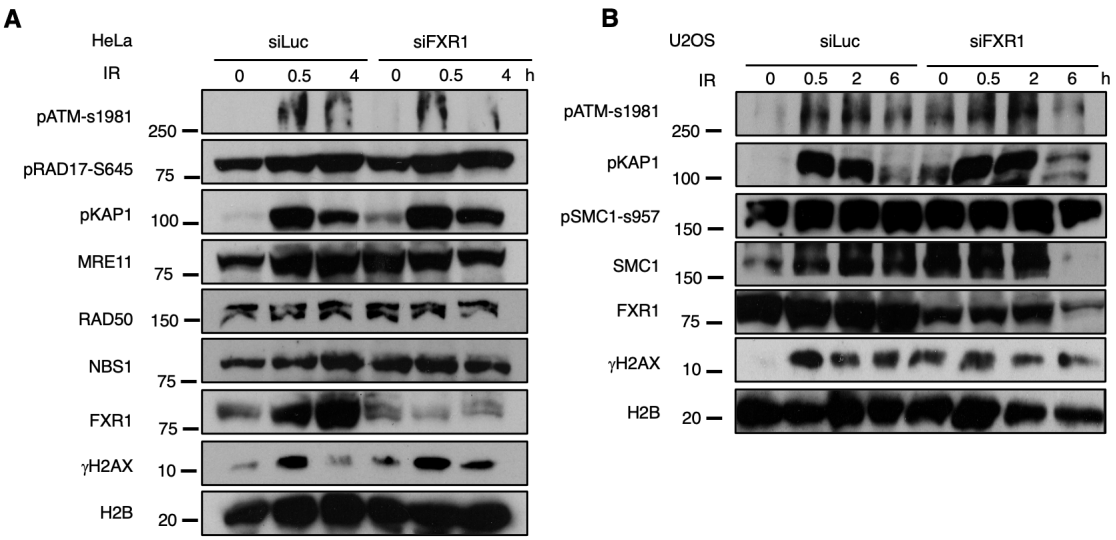

Figure 2.6 FXR1 is dispensable for ATM-dependent phosphorylation. (A) HeLa or **(B)** U2OS cells were transfected by FXR1 siRNA or negative control siRNA, and after 48 h cells were treated with 5 Gy of IR and analyzed by western blot using the indicated antibodies.

I next decided to determine whether FXR1 effect on HR repair activity or not using the DR-GFP assay. When the I-SceI expression plasmid was introduced into U2OS-DRGFP cells to induce DSB injury, the ratio of GFP-positive cells displaying HR activity was not changed in with or without FXR1 knockdown treated cells **(Figure 2.7 A)**. As a marker of HR activation, I examined the accumulation of HR factors by western blotting **(Figure 2.7 B)**. The accumulation of HR factors such as Rad51 and RPA did not increase after irradiation, as most DNA damage by IR is repaired by NHEJ. However, depletion of FXR1 abolished the accumulation of Rad51 and RPA32, both with and without irradiation. Furthermore, when treatment with CPT, a topoisomerase I inhibitor, causes DSBs to repair by the HR pathway, FXR1 knockdown cells showed an increased apoptosis rate of about 6% compared to control cells **(Figure 2.7 C)**. These results

suggested that FXR1 may partially contribute to HR repair in the cellular response to DSB.

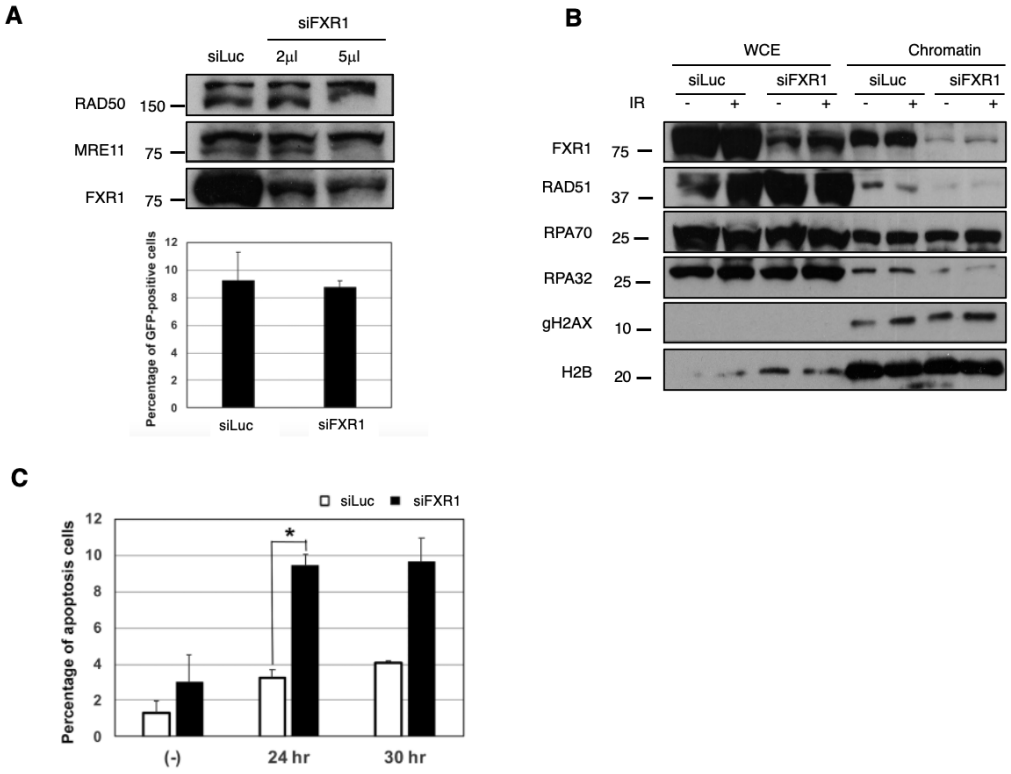

Figure 2.7 FXR1 may partially contribute to HR repair in the cellular response to DSB. (A) U2OS-DRGFP cells were transfected by siRNA targeting FXR1 or luciferase negative control for 48 h, then a DR-GFP assay was performed to measure HR activity. HR activity level was measured as the percentage of GFP-positive cells by flow cytometry. **(B)** U2OS cells were transfected with siRNA targeting FXR1 or luciferase negative control siRNA, and after 2 days these cells were irradiated with 10 Gy of IR. After 4 h cells were harvested and chromatin fractions were prepared. Chromatin accumulation of DDR proteins was detected by western blot analysis using the indicated antibodies. WCE: Whole cell extract. **(C)** HeLa cells were transfected with siRNA targeting FXR1 (close column) or negative control (open column), and after 48 h cells were treated with camptothecin (10 μM), then the percentage of apoptosis in cells was measured by flow cytometry; $* P < 0.05$.

3.3.4 FXR1 participates in the oxidative stress response

I next investigated the role of FXR1 in the oxidative stress response. As ROS are mainly generated by mitochondria, I used the mitochondrial electron transfer inhibitor pyocyanin to induce oxidative stress[78]. In control cells, the oxidative stress pathway was activated, as shown by increased phosphorylation of p38MAPK with pyocyanin treatment for 4 h, and markers associated with ATM-dependent phosphorylation, such as p53 and γH2AX, also increased **(Figure 2.8 A)**. However, these responses were suppressed in FXR1-depleted cells, suggesting that FXR1 might be necessary for oxidative stress responses including the ATM-dependent pathway. I then examined ATLD cells treated with pyocyanin and found that dysfunction of MRE11 perturbed ATM-dependent phosphorylation as well as phosphorylation of p38MAPK **(Figure 2.8 B)**. However, depletion of NBS1 by siRNA did not abolish ATM-dependent phosphorylation in pyocyanin-treated cells **(Figure 2.8 C)**. Finally, if FXR1 is involved in oxidative stress responses, depleting it may sensitize the cells to pyocyanin treatment. To verify this, I analyzed FXR1-depleted U2OS cells treated with pyocyanin. The viability of FXR1-depleted cells was reduced to almost 60% after 24 h of treatment, while in control cells it remained unchanged **(Figure 2.8 D)**. From these results, I infer that FXR1 might play a role in cellular responses against oxidative stress.

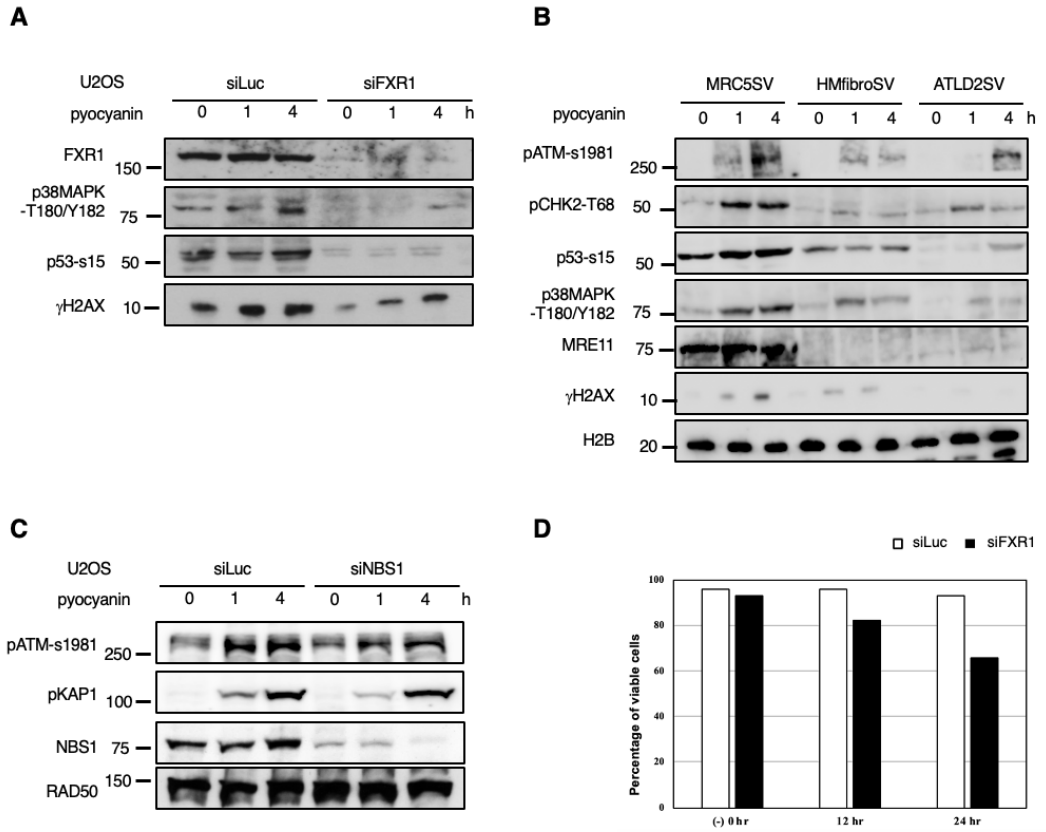

Figure 2.8 FXR1 participates in the oxidative stress responses. (A) U2OS cells were transfected with FXR1 siRNA or negative control siRNA for 48 h, then cells were treated with 50 μM of pyocyanin for the indicated time. Whole cell extracts from the harvested cells were analyzed by western blot using the indicated antibodies. **(B)** MRC5SV and MRE11-defective ATLD cells (HMfibroSV or ATLD2SV) were treated with 50 μM pyocyanin for the indicated time and whole cell extracts from the harvested cells were analyzed by the indicated antibodies. **(C)** U2OS cells were transfected with siRNA targeting NBS1. After 48 h, these cells were irradiated with 50 μM of pyocyanin, harvested for the indicated time, and analyzed by indicated antibodies. **(D)** U2OS cells were transfected by FXR1 siRNA. After 48 h, cells were treated with 100 μM of pyocyanin for the indicated time, and then the cell numbers were counted with a cell counter (BIO-RAD). Open column; negative siRNA; Closed column; FXR1 siRNA.

2.4 Discussion

Both AT and ATLD patients show a similar neurodegeneration phenotype, such as progressive cerebellar ataxia, but the molecular mechanisms of pathogenesis have been elusive. ATM is activated in response to H_2O_2 -induced oxidative stress[33], and defects in its activity were suggested to sensitize neural cells to oxidative stress, leading to ataxia. The role of MRE11 in DDR such as HR repair and the ATM-dependent cell cycle checkpoint has been studied in detail. However, whether MRE11 is associated with oxidative stress responses along with ATM was unknown. Here, I showed that MRE11 but not NBS1 and RAD50 is responsible for ATM activation and ATM-dependent phosphorylation during oxidative stress (**Figure 2.1**). I also identified FXR1 as a novel MRE11-binding partner (**Figure 2.3**) and showed that FXR1 could bind with MRE11 in an NBS1-independent manner (**Figure 2.4**). Furthermore, I found that they localize in the cytoplasm and accumulate in the mitochondrial fraction (**Figure 2.2 C, D; Figure 2.5**). Although MRE11 is an important factor for DNA damage responses, particularly HR repair, FXR1 may partially contribute to HR repair, but not to ATM activation in response to DSB damage (**Figure 2.6-2.8**).

Until now, the functions of MRE11 in the cytoplasm were less characterized. Kondo et al. reported that cytoplasmic MRE11 functions as a sensor of cytosolic double-strand DNA (dsDNA), which is caused by viral or bacterial infection and activates an interferon β-related inflammatory response through the STING pathway[85]. NBS patient cells also show amplification of these responses, suggesting that NBS1 might not be necessary for the detection of cytosolic dsDNA. As NBS cells show cytoplasmic localization of MRE11[84], the functions of cytoplasmic MRE11 could be specific and distinct from its

nuclear functions, such as regulation of HR repair and ATM activation. Remarkably, AT patients and ATM-knockout mice show oxidative stress-related abnormalities in neural cells [50,86,87], and ATLD patients show oxidative stress accumulation in several brain cell types[88]. I show here that MRE11 localizes to mitochondria, where most cytoplasmic ROS are generated. Together, these data support a novel role of MRE11 in the cytoplasm against oxidative stress, through ATM activation.

FXR1 is an RNA-binding protein with high homology to FMR1, the main factor responsible for fragile X syndrome[89]. Both FXR1 and FMR1 directly bind to the Cdc42 effector PAK1 through their KH (2) domain[90]. Cdc42 was reported to participate in the oxidative stress response in cultured neuronal cells[91]. Fragile X syndrome patients show various brain dysfunctions including mental retardation, Parkinson's disease, progressive cerebellar ataxia, and cognition disorder[92]. Moreover, FMR1-knockout mice show mitochondrial fragmentation by impaired mitochondrial fusion and increased oxidative stress in immature neurons[93]. Hence, Fragile X syndrome-related FMR1 and FXR1 might play a role in defense against oxidative stress, possibly through mitochondria, in brain cells. Importantly, I found that depletion of FXR1 reduced oxidative stress-related responses and increased sensitivity to pyocyanin treatment. Moreover, MRE11 might also be indispensable for ATM activation in response to mitochondrial ROS accumulation. Therefore, complex formation between MRE11 and FXR1 may be indispensable for cellular responses against mitochondria-related oxidative stress. The role of FXR1 in the regulation of mRNA turnover through its RNA-binding domain has been reported[94,95]. In FXR1-overexpressing cells, FXR1 bound to and destabilized p21 mRNA, causing a decrease in its levels[95]. Furthermore, depletion of FXR1 in mouse adult neural stem cells caused deficient neural differentiation along with p21

reduction, but restoration of p21 mRNA levels partially rescued this abnormality[96]. MRE11 also shows mRNA-related regulatory roles. Inhibition of transcription progression following damage of template DNA generates R-loop. As this can repress the completion of transcription leading to genomic instability, mechanisms to suppress R-loop also exist[97]. MRE11 was reported to cooperate with the Fanconi anemia pathway for suppression of the R-loop[98]. R-loop accumulation was also reported in brain cells of fragile X syndrome and AOA2, and Senataxin is also associated with R-loop suppression[76]. Although the relationship of FXR1 with R-loop is unknown, accumulation of R-loop in neural cells could contribute to neurodegeneration phenotypes such as cerebellar ataxia. Therefore, the functional interaction between MRE11 and FXR1 in R-loop suppression and their relationship with progressive cerebellar ataxia, in addition to oxidative stress responses, remains to be clarified. As a possible cause of cerebellar ataxia might be related to oxidative stress, I need to clarify in detail the functional interaction between MRE11 and FXR1 in oxidative stress responses. However, their interaction in neural cells should be further investigated, because the sensitivity of neural cells to ROS is different from that of culture cells such as fibroblasts[79,86]. Such research might supply significant clues to clarify the pathogenic mechanisms of other forms of neurodegeneration.

Chapter 3

Exogenous SLFN11 expression suppresses ATR kinase levels in cell fate decision during replication stress response

3.1 Introduction

The *Schalfen (SLFN)* gene family was identified in developing mice thymocytes and the name ("sleep" in German) was coined since they generally prevent cell growth when expressed[99]. The *SLFN* family is mostly mammalian-specific and has undergone rapid diversification probably due to their involvement in the immune response. SLFN11, a long-form member of the SLFN gene family, participates in various biological processes such as anti-viral defense or replication stress response[68,100-102]. In many human cancer and cancer-derived cell lines, the *SLFN11* gene is often silenced and not expressed. Thus, *SLFN11* might function as a tumor suppressor[66]. Loss of SLFN11 rendered cancer cells generally more tolerant to replication stress and DNA damage during anti-cancer drug treatments[103]. Hence, *SLFN11* is critical for cell fate decision following cancer chemotherapy and is now proposed to be a potential biomarker to predict clinical outcomes following chemotherapy[104,105]. However, how the expression of *SLFN11* mechanistically affects cancer development and facilitates cell death after DNA damage remains to be established. The long-form SLFNs (including SLFN11) harbor two functional modules: the N-terminal core domain containing ribonuclease features and the C-terminal helicase/ATPase domain[102]. To understand how SLFN11 can affect the biological behavior of cancer cells, it might be important to elucidate the role of these domains and whether they are functionally inter-connected.

The C-terminal helicase domain has been reported to mediate cell fate decisions in response to DNA damage and replication stress. It has been well established that stalled replication forks are reversed by the actions of fork remodeling enzymes such as SMARCAL1, resulting in a 4-way junction structure which is subjected to digestion by

nucleases like DNA2 and MRE11. Fork degradation must be tightly regulated for resumption of replication, and hence, cell survival[106]. Our lab has previously implicated the role of *SLFN11* in accelerating stalled fork degradation, by preventing recruitment of the fork protector RAD51[107]. I proposed that this fork instability may be the basis for enhanced DNA damage sensitivity by SLFN11[107]. Several additional mechanisms have been suggested to enhance DNA damage sensitivity: *SLFN11* suppresses DNA repair activity due to homologous recombination and affects checkpoint maintenance[108], blocks replication fork progression[109], or promotes the degradation of the replication factor CDT1[110].

In contrast, it was also shown that SLFN11 RNase activity downregulates protein levels of ATR kinase, which is critical for the cellular response to DNA damage and replication stress, thereby decreasing viability following DNA damage[111]. ATR accumulates at the stalled forks by binding to RPA via its subunit ATRIP and is activated through binding with the ATR-activating domain of TopBP1 or ETAA1[38]. ATR phosphorylates its substrates, which are crucial for downstream checkpoint and replication stress responses. Li et al. reported that the codon usage of ATR is distinct and its translation depends on a specific subset of tRNAs, which are the target of SLFN11 RNase activity[111]. Consistent with this idea, it is well established that the RNase domain of SLFN family members is involved in translational regulation by cleaving tRNA/rRNA as an endonuclease and exerting anti-HIV activity, which is present in hSLFN13 [112] as well as in hSLFN11[113,114].

It is difficult to reconcile these two lines of evidence each depending on the N-terminal RNase domain and C-terminal helicase domain, respectively. In this study, I planned to obtain insights into the role of the SLFN11 RNase domain in the replication stress

response. Based on the structural and biochemical data in the literature[112,115], a *SLFN11* RNase domain mutant, in which two functionally critical residues were both changed to alanine was made, and expressed this mutant in HAP1 *SLFN11*$^{-/-}$ cells (by our lab member Ms. Erin Alvi). Our analysis revealed that the RNase domain mutant can suppress cell survival following hydroxyurea (HU) treatment and destabilize stalled replication forks similarly to wild-type SLFN11(Erin, revision). Nucleases (i.e., DNA2 and MRE11) were similarly promoted for digestion by the RNase domain mutant. Not unexpectedly, a novel MRE11 interactor FXR1 (FMR1 autosomal homolog 1) which I have previously identified[116], was dispensable. Surprisingly, I also found that ATR kinase levels were markedly downregulated by the expression of both wild-type and the RNase mutant SLFN11. To look at the similarity between the effect of reduced ATR levels and SLFN11 expression, I employed ATR inhibitor (ATRi) treatment and observed that ATRi phenocopied the cells with exogenous SLFN11 expression regarding the stalled fork degradation. Given the previous reports showing that ATRi, or lower ATR levels, can generally potentiate DNA damage sensitivity and reduce RAD51 foci formation (for example, see[117]), I propose that a critical role of SLFN11 in cancer chemotherapy may involve the regulation of ATR levels independently of its RNase activity.

3.2 Method and materials

3.2.1 Cell culture

HAP1 cells were derived from the human haploid chronic myelogenous leukemia (CML) cell line KBM-7 and cultured in IMDM (Nacalai Tesque) supplemented with 10% Fetal Bovine Serum (FBS). HEK293T cells were cultured in DMEM-high glucose (Nacalai Tesque) supplemented with 10% FBS.

3.2.2 Drug treatment

Cells were treated with Hydroxyurea (HU) (Millipore Sigma) at the indicated concentrations and time as described in the figures. For ATR kinase inhibit experiments, cells were incubated with 1 μM of VE-821(Toronto Research Chemicals) together with drug treatment. Doxycycline (DOX) was used for *SLFNs* expression, cells were incubated with 2 μg/ml for 48 h before drug treatment.

3.2.3 Generation of the RNase deficient SLFN11 mutant

The wild-type *SLFN11* coding sequence cloned in pENTR plasmid is mutated by inverse PCR (forward 5'-CGTCTCAGTTAGTAGCGTTTAAACAGTTCT-3', reverse 5'-GCTACTAACTGAGACGCAGGAAAAGGCAGG-3'; Invitrogen), and confirmed by Sanger sequencing. The mutated *SLFN11* was transferred by the Gateway system using Clonase II (Invitrogen).

3.2.4 Lentivirus transduction in *SLFN11*$^{-/-}$ HAP1 cell line

To express *SLFNs* under tetracycline-controlled transcriptional activation, lentivirus was generated. HEK293T cells were first cultured in 6-well plates with 2 mL DMEM medium. Transfections were carried out with the Lipofectamine 3000 reagent according to the manufacturer's instructions. The CSIV(RIKEN) plasmid with the gene of SLFN 11 and SLFN11 RNase mutant (1.9 μg) was transfected with the lentivirus packaging plasmids pCAG HIV gp (1.1 μg), pCMV-VSV-G-RSV-Rev (1.1 μg). HEK293T cells were collected, then cells were seeded in a 6-well dish with a total of 2 mL DMEM at a concentration of 0.5× 10^6 cells. 125 μL of Opti-MEM was added into each tube that contained the plasmids. All three plasmids were added to each tube with 5 μL of P3000 enhancer, vortex, and incubated at RT for 2 min. 125 μL of the lipofectamine reagent diluted in Opti-MEM was added to the plasmid tubes, vortexed, and incubated at RT for 5 min. The mixture was added to wells and incubated for 48 h.

The day before collecting the virus, 2500 HAP1 *SLFN11*$^{-/-}$ cells/well were seeded in a 24-well plate containing 300 μl IMDM for 4 wells. HEK293T cells were collected and centrifuged at 1200× g for 5 min. The medium was carefully passed through a 0.22 μm filter to catch cells and debris. 500 μl of the medium containing the virus, was then applied to the *SLFN11*$^{-/-}$ HAP1 cells in the 24-well plate. After incubating for 48 h infected with viral supernatants, cells were transferred into a 10 mL dish for selection with 400 μg/mL hygromycin (Nacalai Tesque). Single clones were isolated and verified by western blotting. *SLFNs* expression was induced by treatment with 2 μg/ml doxycycline (DOX) for 48 h (made by our previous lab member Erin).

3.2.5 Small interfering RNA (siRNA) transfection

Endogenous DNA2, MRE11, and FXR1 in HAP1 cells were knocked down by siRNAs. Transfection was carried out using Lipofectamine RNAi Max (Invitrogen). After 72 h, cells were collected and performed western blotting analysis and DNA fiber assay. The individual siRNA duplexes used were as follows:

Table 3.1 sequences of duplexes

siRNA	Sense strand	Source
siDNA2	5'-CAUCCAAUAUUUUCCCGUA-3'	Millipore Sigma
siMRE11	5'-GAUGAGAACUCUUGGUUUATT-3'	B-Bridge International Inc
siFXR1	5'-GGUUCGAGUGAGAAUUGAATT -3'	Qiagen Co
siControl	5'-UCGAAGUAUUCCGCGUACGTT-3'	Millipore Sigma

3.2.6 Cell growth assay and cytotoxicity assay

For cell growth assay, HAP1 cells (1×10^5) were seeded into 6 cm dishes at day 0 and counted every 24 h. For cytotoxicity assays, HAP1 cells (2.5×10^3) were plated in a 96-well plate in a quadruplicate for each condition. After 48 h of DOX pre-treatment (*SLFN11* transduced cells), the indicated concentration of HU was added to the wells and incubated for an additional 72 h. Cell viability was measured using a Cell Counting Reagent SF (Nacalai Tesque). Absorbance at 450 nm was measured with a Multilabel Reader (PerkinElmer).

3.2.7 Immunoblotting

After the drug treatment, cells were harvested and washed with PBS twice. The cells were lysate with 1X SDS buffer (containing 2-mercaptoethanol) at a final concentration of $5x10^6$cells/ml, then performed sonication for 10 min. After centrifugation, the lysate was boiled at 95°C for 5 min. 10 μl of protein extracts was separated by sodium dodecyl sulfate-polyacrylamide gel electrophoresis (SDS-PAGE) or Extra PAGE One Precast Gel (Nacalai Tesque) SDS-PAGE gel for 2 h. Electrophoresed proteins were transferred to polyvinylidene difluoride (PVDF) membrane at 15V (constant voltage condition) at room temperature for 0.5hr. The transferred membrane was gently shaken in a blocking solution (5% skim milk/TBST) at room temperature for 1h. The membrane was washed gently with TBST. Then, the membrane was reacted with primary antibody, diluted by skim milk/TBST at 4 ℃ overnight. After the reaction of the primary antibody, the membrane was washed with TBST for 10 min three times and then reacted with the secondary antibody, for 1h at room temperature. After the reaction of the secondary antibody, the membrane was washed with TBST for10 min 3 times. The membrane was reacted with ECL plus chemiluminescence system (GE Healthcare) for 5min at room temperature, then target proteins were visualized with Image Quant LAS 4000mini.

3.2.8 Reverse-transcription PCR assay

Total RNA was extracted using RNeasy Plus Mini Kit (QIAGEN, # 74134). PrimeScript™ RT reagent kit with gDNA Eraser (TaKaRa) was used for the first-strand cDNA synthesis with 1 μg total RNA. PCR amplification was carried out using KOD-FX polymerase (TOYOBO) with gene-specific primers shown in Table 2.2. The experiments

were carried out according to the manufacturer's instructions with PCR conditions used: 94℃ for 2min, 30 cycles at 98℃ for 10sec, and 68℃ 1min./kb.

Table 3.2 Primer sequences for RT-PCR analysis

Target gene	Primer sequence	Number
hATR	Forward:5'-GCTGGTTTGAGACCTATTCTGAC-3'	KD8-183
	Reverse:5'-CATATATGGAGTCCAACCAAGATAC-3'	KD8-148
hGAPDH	Forward: 5'-ACCCAGAAGACTGTGGATGG-3'	KD16-30
	Reverse:5'-TTCTAGACGGCAGGTCAGGT-3';	KD16-31

3.2.9 DNA fiber assay

HAP1 cells were cultured at about 80% confluent for the experiment. Cells were firstly labeled with 25 μM IdU for 30 min, then washed with cold PBS twice, and secondary labeled with 250 μM CldU for another 30 min. Subsequently, cells were treated with or without 4 mM HU for 5 h. Cells were collected and suspended in 70% ethanol at a final concentration of 5 x 10^5 cells/ml. After spotting 2 μl of the cell suspension onto glass slides, cells were lysed with 8μl lysis buffer with a mixture of 50 mM EDTA, 0.5% SDS, and 200 mM Tris-HCl (pH 7.5); and mixed using a circular motion with the pipette. Tilting the slides at 15° to spread the DNA across the slide, and dry up at 4℃ overnight. Fibers were fixed in a solution of methanol: acetic acid (3:1) in a staining jar. Then, 2.5 M HCl was used to denature for 60 min, and the slides were washed in PBS 3 times.

The slides are blocked using Blocking One (Nacalai Tesque) for 20 min before incubating with the first antibody. The primary antibodies used were anti-BrdU from BD (for IdU, mouse) and anti-BrdU from Abcam (for CldU, rat) diluted to 1:400 in Blocking

One, added to slides for 1 h in a humidified chamber, and protected from light. The slides are washed with PBS-T 3 times before incubation with the secondary antibodies. The secondary antibodies are anti-mouse Alexa594 and anti-rat Alexa488 in a 1:500 dilution, and after adding ~200 μL to each slide they are incubated for 1 h in the humidified chamber, protected from light. Finally, slides are washed with PBST and PBS, then a mounting medium (Prolong gold antifade reagent, Invitrogen) is added and topped with cover glass, then sealed with nail polish to protect the slides. Fibers labeled with IdU (red) then CldU (green) were measured using the Leica DM5500B microscope and Leica Application Suite X (LAS X) software. The degradation of nascent DNA (second tract length) of each sample was analyzed with Prism software.

3.2.10 Protein sequence alignments

To analyze homology between the protein sequences of each SLFN of interest, NCBI protein sequences (hSLFN11: NP_001098057.1; hSLFN13: NP_653283.3; hSLFN5: NP_659412.3; mSLFN8: NP_853523.2; mSLFN9: NP_766384.2; rSLFN13:NP_00101399.1;) were used and a MAFFT alignment was performed using Genetyx software (GENETYX Corp. Tokyo, Japan).

3.2.11 Statistical analysis

Statistical analysis was performed using Prism software (version 9). One-way analysis of variance (ANOVA) was used for Tukey's multiple comparisons. Data are expressed as mean ± SD, and differences are assessed as ns =not significant, ***p< 0.0001).

Table 3.3 Antibodies for immune blotting analysis

Antibodies	Catalog	Source
SLFN11(E4)	374339	Santa Cruz Biotechnology
DNA2	ab96488	Abcam
phospho-CHK1(s345)	2341	Cell Signaling Technology
phospho-ATR(T1989)	58014	Cell Signaling Technology
phospho-RPA32 (Ser33)	a300-246a	Bethyl
ATR	ab2905	Abcam
MRE11	GTX70212	Genetex
FXR1	a303-892a	Bethyl
RPA2 (9H8)	ab2175	Abcam
tubulin	T5168	Millipore
IdU	347580	BD Biosciences
CldU	ab6326	Abcam

3.3 Results

3.3.1 SLFN11 enhances cellular sensitivity to DNA-damaging reagents independent of its RNase domain.

Previous works by our lab member Dr. Yusuke Okamoto and others indicated that *SLFN11* enhances DNA damage sensitivity via its C-terminal helicase domain. However, the SLFN11 protein also has an N-terminal core domain which acts as a ribonuclease (RNase) for a specific subset of tRNA/rRNA [112,114,115] and is engaged in translation control of ATR kinase[111]. Therefore, I decided to investigate whether the RNase domain of SLFN11 is responsible for affecting DNA damage sensitivity or not. To this aim, two inactivating mutations on the critical residues in the RNase domain in the N-terminal SLFN11 core domain was introduced (by Ms. Erin Alvi) (**Figure 3.1A and B**) and tested whether the expression of SLFN11 with the RNase domain mutations could restore the phenotype caused by the loss of human *SLFN11* in human HAP1 cells [107]. These two residues are very well conserved among SLFN family members and are shown to be critical for tRNA cleavage by rat or human SLFN13[112] and hSLFN11[114]. HAP1 *SLFN11*$^{-/-}$ cells were infected with lentivirus vectors encoding DOX-inducible GFP-tagged wild-type SLFN11(+SLFN11 WT) or RNase domain mutant SLFN11(+SLFN11 RNase mut). The expression of SLFN11 in the clones selected by hygromycin was confirmed following 48 h induction of DOX treatment with immunoblotting using an anti-SLFN11 antibody (**Figure 3.1C**).

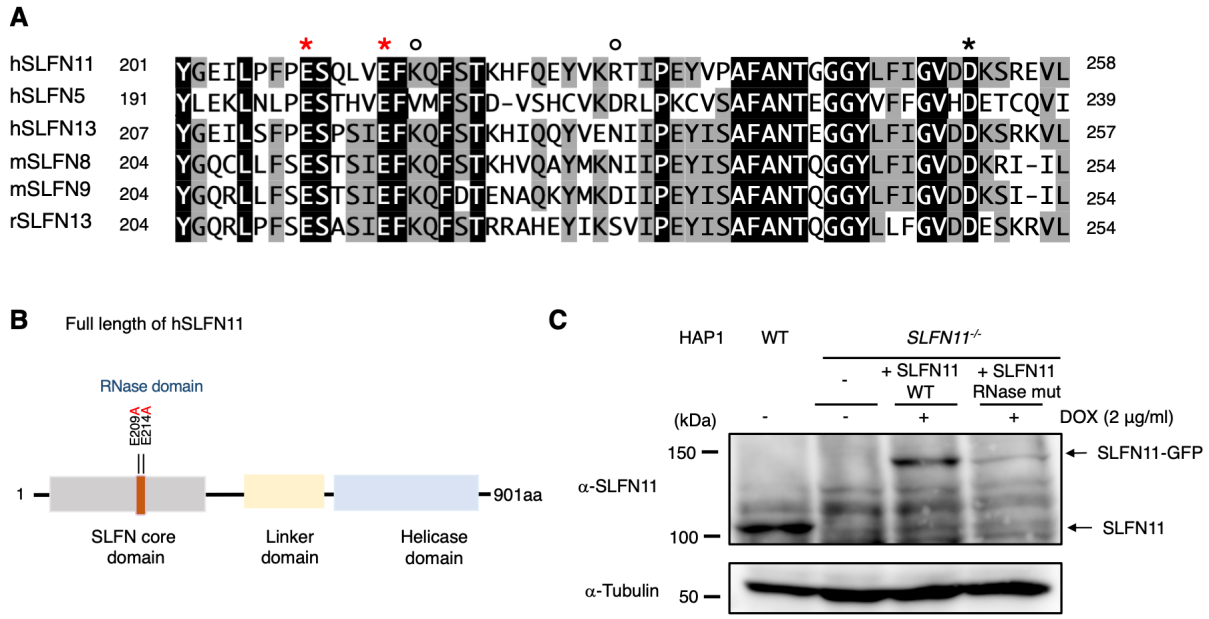

Figure 3.1 Expression of wild-type and RNase mutant SLFN11 in *SLFN11*$^{-/-}$ HAP1 cells. (A) Multiple sequence alignments of the proposed active site regions of selected Schlafen proteins. The critical catalytic residues are indicated with E/D = *, K/R = o. The method used for alignment was the MAFFT program (Genetyx-Mac). The conserved regions were from the Pfam database. **(B)** A schematic diagram of SLFN11 protein structure. Positions of the mutation in the ribonuclease domain are shown. **(C)** Western blots (WB) analysis of DOX-induced expression of SLFN11. HAP1 *SLFN11*$^{-/-}$ cells were transduced with GFP tagged wild-type SLFN11 or the ribonuclease mutant SLFN11. Lentivirally transduced cells were treated with 2 µg/ml doxycycline (DOX) for 48 h for expression.

I firstly assessed the proliferation of cells expressing wild-type SLFN11 or the RNase domain mutant. It has been reported that *SLFN11*-depleted cells proliferated significantly faster than wild-type HAP1 cells[107], and the exogenous *SLFN11* expression decreased cell growth rate[107]. Indeed, I observed that the *SLFN11*$^{-/-}$ HAP1 cells grew faster than the wild-type HAP1 cells (**Figure 3.2**), and the expression of both wild-type and the RNase domain mutant similarly decreased growth rate (Figure 3.2).

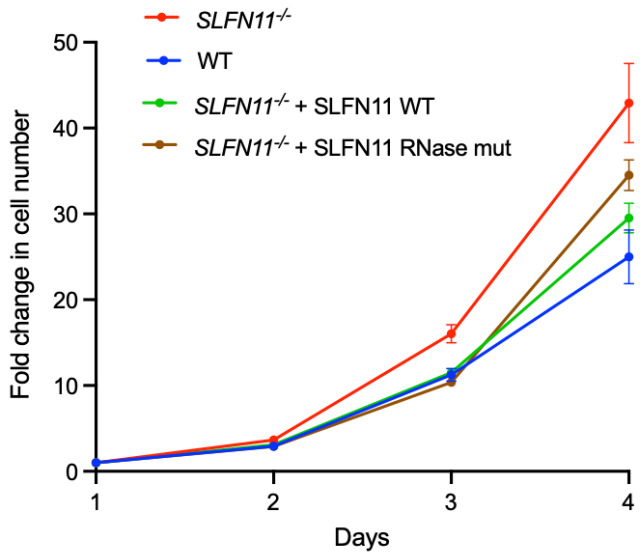

Figure 3.2 Cell proliferation profile of *SLFN11*$^{-/-}$ HAP1 cells with indicated transgenes. Fold change in growth was measured over 4 days in wild-type or *SLFN11*$^{-/-}$ HAP1 cells complement with SLFN11 or RNase mutant SLFN11. Data represent mean ± SD.

Hydroxyurea (HU), a ribonucleotide reductase inhibitor, causes depletion of the deoxynucleotide pool in the cell, thereby inducing replication stress and stalled replication forks. I investigated whether SLFN11 with mutations in the RNase domain affects cellular sensitivity to HU. Consistent with the previous findings[107], I observed that DOX-induced wild-type SLFN11 expression in HAP1 cells partially restored cellular sensitivity to HU (**Figure 3.3**). Furthermore, expression of the RNase domain mutant SLFN11 also increased cellular sensitivity to HU (**Figure 3.3**), suggesting that the RNase domain of SLFN11 is dispensable for its function in reversing cellular sensitivity to DNA-damaging reagents.

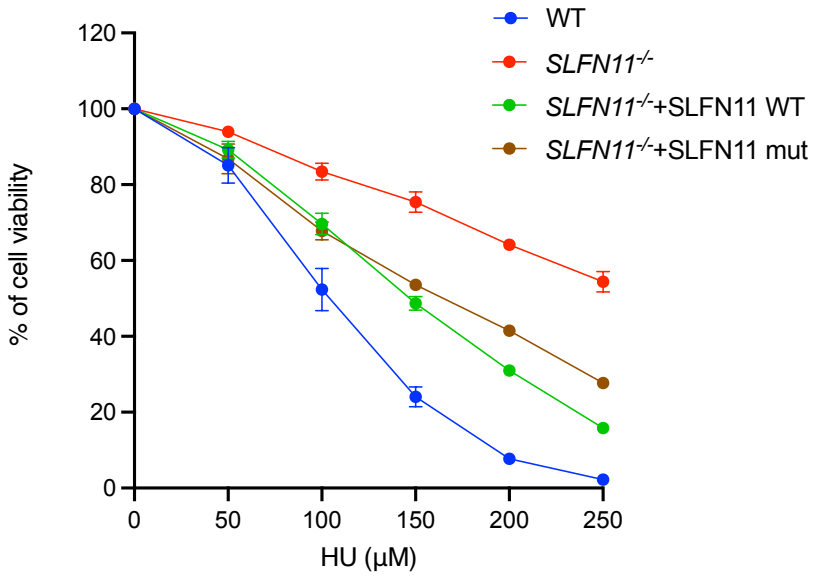

Figure 3.3 Cell survival assay of HAP1 cells. HAP1 cells with indicated genotypes were treated with indicated doses of hydroxyurea (HU) for 72 h and measured with Cell Counting Reagent. Data represent mean ± SD.

3.3.2 SLFN11 accelerates replication fork degradation in a manner independent of its RNase domain

Our lab previously reported that *SLFN11* prevents the recruitment of the fork protector RAD51 to nascent DNA sites during replication stress, thereby accelerating stalled fork degradation[107]. To test whether the SLFN11 RNase domain plays a crucial role in accelerating HU-induced fork degradation, I utilized the DNA fiber assay. Progressing replication forks in HAP1 cells were pulse-labeled with thymidine analogs, 5-iodo-2'-deoxyuridine (IdU) followed by 5-chloro-2'-deoxyuridine (CldU) then exposed to 4 mM HU for 5 h to stall progressing replication forks **(Figure 3.4A, upper)**. The tract length of CldU-labeled DNA was assessed as an index of nascent DNA degradation in a blinded manner. Consistent with the previous findings[107], I observed that the length of CldU tracts in wild-type HAP1 cells were shortened (degraded) following HU treatment, while there were no significant changes in the CldU tract lengths of *SLFN11*$^{-/-}$ HAP1 cells with and without HU treatment (**Figure 3.4A and B**). I further carried out DNA fiber assays in *SLFN11*$^{-/-}$ HAP1 cells complemented with wild-type *SLFN11* or the RNase domain mutant. I found that re-expression of wild-type SLFN11, as well as the RNase domain mutant, significantly shortened CldU tract length during HU treatment, suggesting that the RNase domain was not required for accelerating nascent replication fork degradation (**Figure 3.4A and B**).

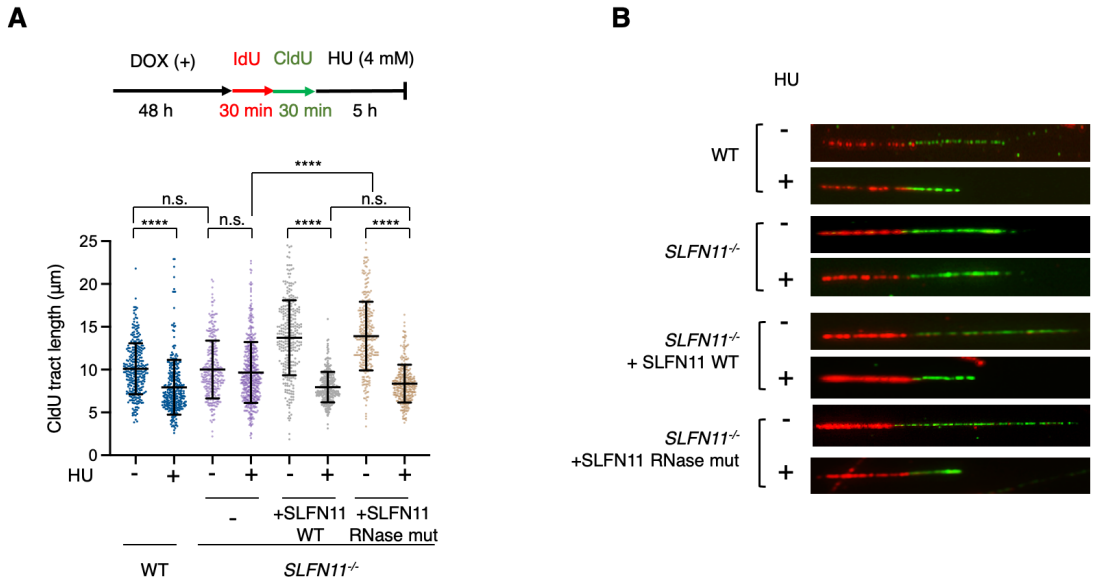

Figure 3.4. Expression of *SLFN11* with a mutated ribonuclease domain accelerates the degradation of stalled replication forks. (A) A schema of the experimental protocol (upper). Quantification results of fork degradation in HAP1 cells with the indicated genotypes in the presence of HU (below). The CldU tract length of over 300 DNA fibers were measured in each sample. To minimize the effects of observer bias, the images were captured and analysed in a blinded manner. P values were calculated by one-way ANOVA with Tukey's multiple-comparisons test. Mean ± SD are shown. n.s., not significant. ****, $p<0.0001$. **(B)** Representative DNA fiber images of HAP1 cells with indicated genotypes.

3.3.3 Expression of SLFN11 carrying the mutated RNase domain enhances degradation of replication forks in a manner dependent on nuclease DNA2 or MRE11

It has been reported that nucleases such as DNA2 and MRE11 participate in digestion of nascent DNA of stalled replication forks during HU treatment[118]. Our previous research indicated that SLFN11 promotes fork degradation in combination with nucleases including DNA2 or MRE11[119]. I performed a DNA fiber assay to test whether the RNase domain mutation could affect this process. I confirmed that siRNA targeting DNA2 in both wild-type and *SLFN11*$^{-/-}$ HAP1 cells successfully decreased DNA2 expression levels with western blotting (**Figure 3.5A**). I then observed that DNA2 knockdown could increase the CldU tract length in wild-type as well as *SLFN11*$^{-/-}$ HAP1 cells re-expressing wild-type SLFN11 post-HU treatment but could not further elongate the tract length in *SLFN11*$^{-/-}$ HAP1 cells (**Figure 3.5B**). As expected, DNA2 knockdown also prevented shortening of the tract length in *SLFN11*$^{-/-}$ HAP1 cells expressing the RNase mutant SLFN11 (**Figure 3.5B**).

Furthermore, MRE11 knockdown efficiency was confirmed by western blotting (**Figure 3.6A**) and showed a similar tendency to DNA2 knockdown in HAP1 cells with each genotype (**Figure 3.6B**), indicating that both DNA2 and MRE11 are crucial for fork degradation that is promoted by SLFN11.

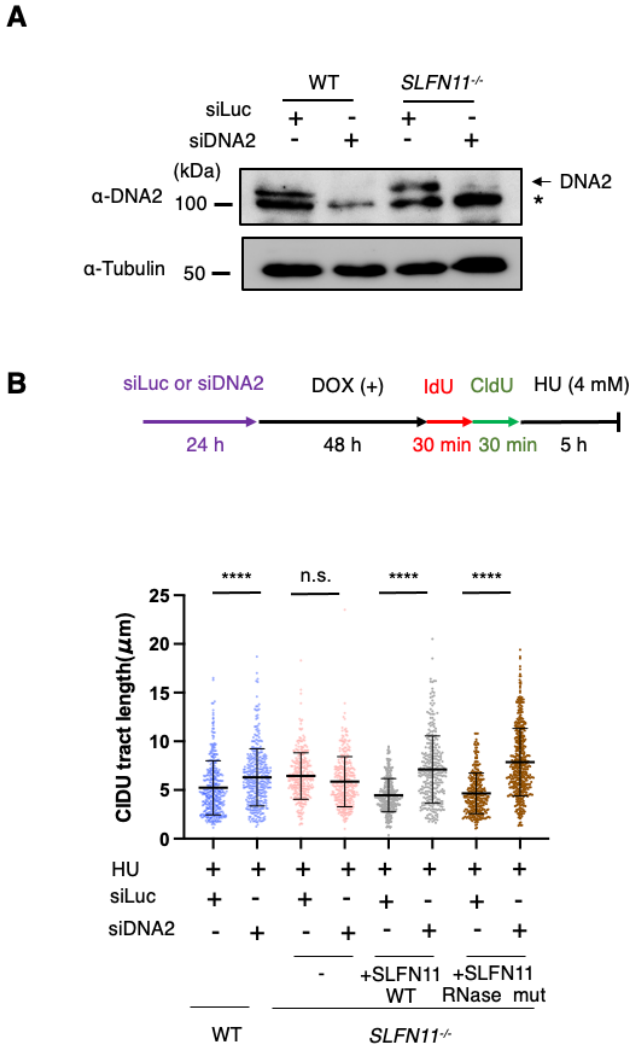

Figure 3.5 DNA2 is responsible for the cleavage of nascent DNA tracts. (**A**) DNA2 depletion by siRNA in the wild-type and *SLFN11*$^{-/-}$ HAP1 cells was confirmed by western blotting analysis. Cells were collected 72 h after transfection with siRNA. Asterisks (*) represents a non-specific band. **(B)** DNA fiber assay results in HAP1 cells. A schema of DNA fiber assay protocol (upper) is shown. Cells were treated with luciferase negative control (siLuc) or siRNA targeting DNA2 for 24 h before DOX-induced expression of wild-type SLFN11 or RNase mutant SLFN11, then exposed to 4 mM HU for 5 h. The length of more than 300 fibers were measured in each sample. P values were calculated by one-way ANOVA with Tukey's multiple-comparisons test. Mean ± SD are shown. n.s., not significant. ****, $p<0.0001$.

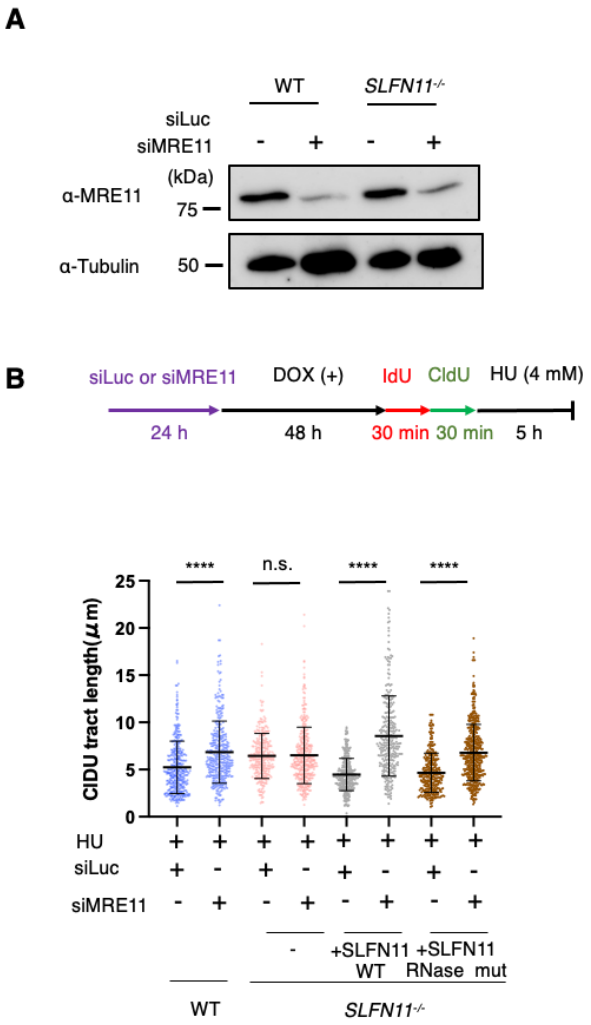

Figure 3.6 MRE11 is responsible for the cleavage of nascent DNA tracts. (**A**) MRE11 depletion by siRNA in the wild-type and *SLFN11*$^{-/-}$ HAP1 cells was confirmed by western blotting analysis. Cells were collected 72 h after transfection with siRNA. Asterisks (*) represents a non-specific band. **(B)** DNA fiber assay results in HAP1 cells. A schema of DNA fiber assay protocol (upper) is shown. Cells were treated with luciferase negative control (siLuc) or siRNA targeting MRE11 for 24 h before DOX-induced expression of wild-type SLFN11 or RNase mutant SLFN11, then exposed to 4 mM HU for 5 h. The length of more than 300 fibers were measured in each sample. P values were calculated by one-way ANOVA with Tukey's multiple-comparisons test. Mean ± SD are shown. n.s., not significant. ****, $p<0.0001$.

3.3.4 Expression of SLFN11 carrying a mutated RNase domain enhances degradation of replication forks in a manner independent of FXR1

In chapter 2, I identified FXR1(FMR1 autosomal homolog 1), an RNA-binding protein, as a novel MRE11 interactor[116]. It could bind with MRE11 in mitochondria and contributes to cellular defense against mitochondrial reactive oxidative stress. To test whether FXR1 acts in fork degradation, I performed the DNA fiber assay in *FXR1*-depleted HAP1 cells (**Figure 3.7A and B**). However, I observed that the FXR1 knockdown did not significantly affect fork degradation in any of the genotypes tested (**Figure 3.7B**). Taken together, these results suggest that SLFN11 promotes replication fork degradation in a manner dependent on nuclease DNA2 and MRE11, but not FXR1. Our data further indicate that the RNase domain of SLFN11 is dispensable for the acceleration of stalled fork degradation.

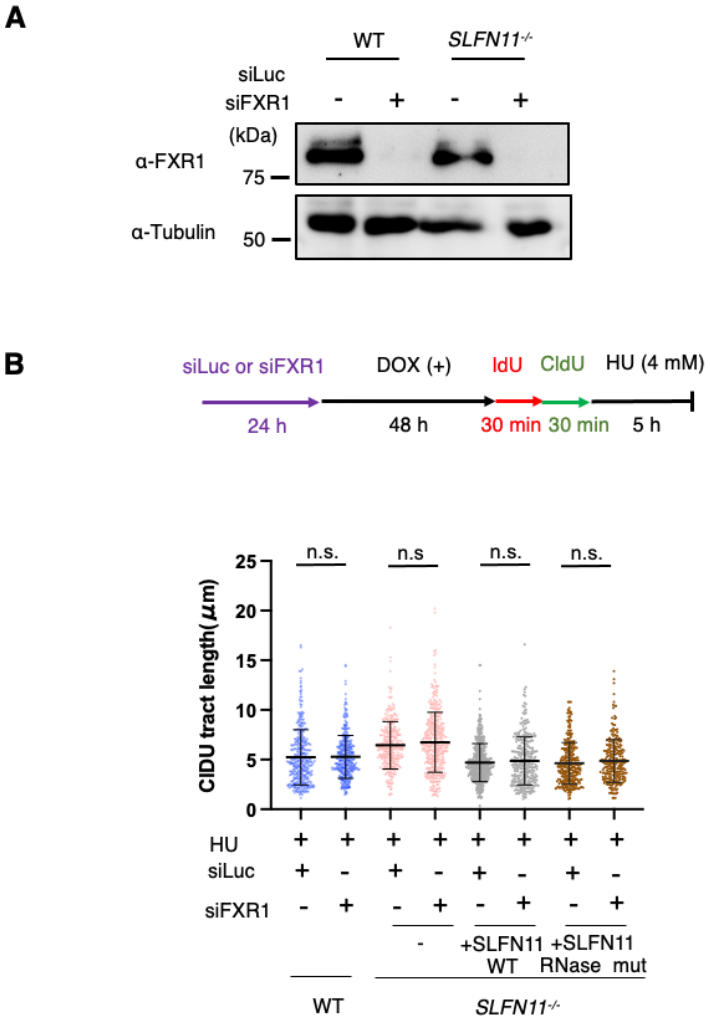

Figure 3.7 FXR1 is dispensable for cleavage of nascent DNA tracts. (**A**) FXR1 depletion by siRNA in the wild-type and *SLFN11*$^{-/-}$ HAP1 cells was confirmed by western blotting analysis. Cells were collected 72 h after transfection with siRNA. Asterisks (*) represents a non-specific band. **(B)** DNA fiber assay results in HAP1 cells. A schema of DNA fiber assay protocol (upper) is shown. Cells were treated with luciferase negative control (siLuc) or siRNA targeting FXR1 for 24 h before DOX-induced expression of wild-type SLFN11 or RNase mutant SLFN11, then exposed to 4 mM HU for 5 h. The length of more than 300 fibers were measured in each sample. P values were calculated by one-way ANOVA with Tukey's multiple-comparisons test. Mean ± SD are shown. n.s., not significant. ****, $p<0.0001$.

3.3.5 Exogenous expression of SLFN11 downregulates ATR kinase expression in response to DNA-damaging reagent-induced replication stress

It has been previously described that SLFN11 inhibits the translation of ATR kinase through cleavage of specific types of tRNA during the DNA damage response, due to the distinct codon usage in ATR[111]. Because this report is apparently at odds with my current observation, I decided to investigate whether SLFN11 expression could affect the expression and function of ATR kinase in response to HU-induced replication stress in HAP1 cells. Western blot analysis confirmed that ATR protein expression did not change with or without HU treatment (5 h) in wild-type HAP1 cells (**Figure 3.8**). In *SLFN11*$^{-/-}$ cells, the basal levels of ATR were slightly lower but were increased to similar levels as wild-type cells after HU treatment, and the auto-phosphorylation of ATR on the Thr1989 residue[120]reached higher levels after HU treatment than in HU-treated wild-type cells. This could reflect higher RPA foci levels in the absence of SLFN11, which may recruit more of the ATRIP-ATR complex to damaged chromatin. However, a bit surprisingly, *SLFN11*$^{-/-}$ cells lentivirally transduced with SLFN11-GFP wild type or the RNase mutant revealed lower levels of ATR kinase than non-transduced *SLFN11*$^{-/-}$ cells. I confirmed the reproducibility of this observation in three repeated experiments.

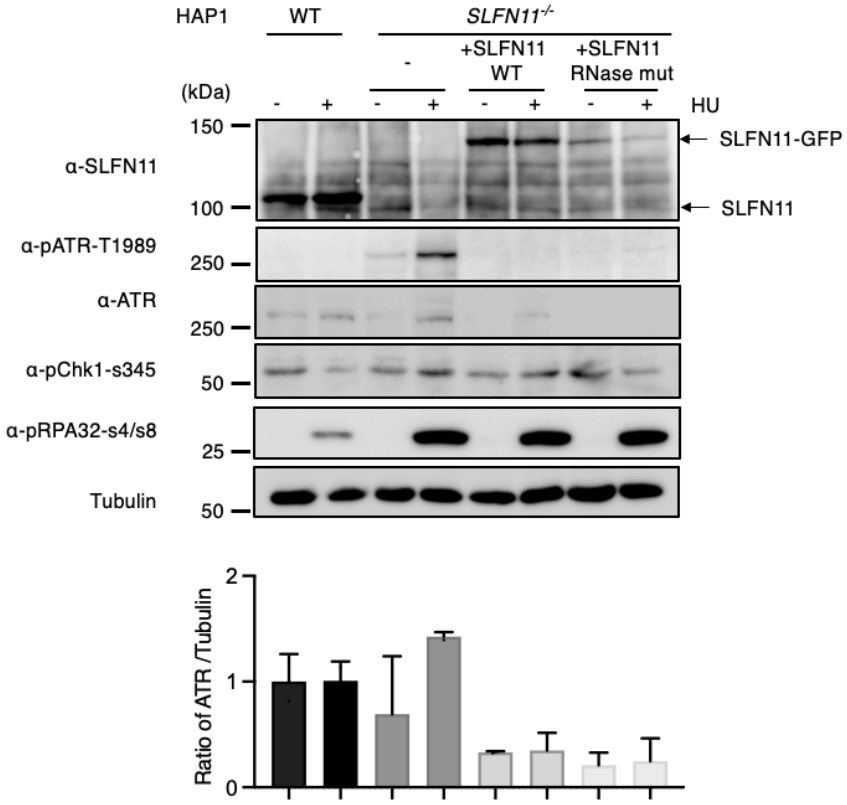

Figure 3.8 Expression of SLFN11 downregulates ATR protein levels in response to HU. HAP1 cells with indicated genotypes were treated with 4 mM of HU for 5 h. Then, the cells were harvested and analyzed by western blotting using the indicated antibodies. Relative expression of ATR was analyzed by Image J and normalized with Tubulin expression.

RT-PCR analysis did not reveal decreased ATR mRNA levels, suggesting a reduction at the protein level (**Figure 3.9**). In keeping with this, the phosphorylation of ATR was barely detectable following HU treatment. The phosphorylation levels of CHK1 on S345, which is known to be phosphorylated by ATR, did not show much difference after HU

treatment between cells expressing wild-type and RNase mutant SLFN11. The Ser4/Ser8 phosphorylation of RPA, which is mediated by DNA-PKcs[121], was increased in *SLFN11*$^{-/-}$ cells compared to wild-type following HU treatment, and exogenous expression of SLFN11 did not reduce these phosphorylation levels (**Figure 3.8**). Overall, these results indicated that exogenous SLFN11 inhibits ATR kinase expression and this effect is independent of its RNase domain.

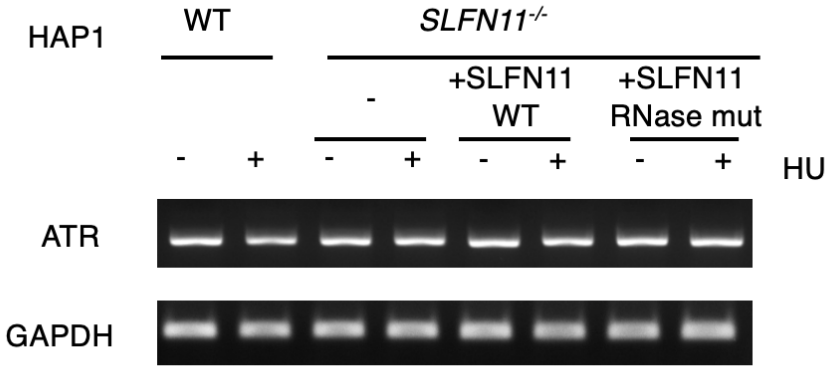

Figure 3.9 ATR mRNA expression in HAP1 cells. The mRNA expression of ATR in HAP1 wild-type and *SLFN11*$^{-/-}$ cells complemented with wild-type or RNase mutant SLFN11 after 4 mM HU treatment for 5 h were analyzed by reverse transcription-PCR (RT-PCR).

3.3.6 ATR inhibition mimicked the effects of SLFN11 expression in stalled fork degradation

My observation that exogenous expression of SLFN11, irrespective of RNase domain mutations, suppressed ATR kinase levels suggested that lower functional levels of ATR might explain the effects of exogenously expressed SLFN11 during replication stress and in the DNA damage response. To test whether ATR inhibitor (ATRi) treatment can simulate SLFN11 expression, I treated *SLFN11*$^{-/-}$ HAP1 with ATRi VE-821 and examined the degradation of nascent DNA tracts with and without HU treatment. Similarly to the observation in *SLFN11*$^{-/-}$ complemented with SLFN11, I could detect enhanced stalled fork degradation in ATRi-treated *SLFN11*$^{-/-}$ cells (**Figure 3.10)**, consistent with the possibility that the effects of exogenous SLFN11 expression on fork degradation are mediated by suppressed expression and function of ATR kinase.

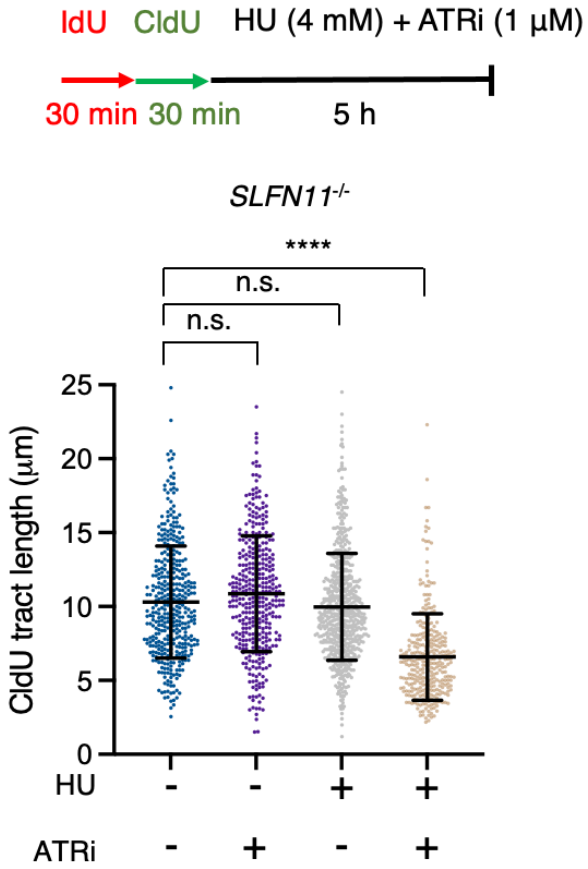

Figure 3.10 DNA fiber assay following ATR inhibitor treatment in HAP1 *SLFN11*$^{-/-}$ cells. 1 μM ATR inhibitor (VE-821) was applied to cells together with HU (upper). The length of more than 300 fibers were shown. P values were calculated by one-way ANOVA with Tukey's multiple-comparisons test. Mean ± SD are shown. n.s., not significant. ****, $p<0.0001$.

3.4 Discussion

There are two conflicting views in the literature on the mechanisms of SLFN11-mediated enhanced DNA damage sensitivity, which seem difficult to reconcile. While the C-terminal helicase domain of SLFN11 is proposed to modulate DNA metabolism such as DNA repair[108] or replication[109,110], the N-terminal RNase domain is suggested to downregulate translation of critical replication stress kinase ATR, leading to loss of checkpoint response[111]. In this study, I provide lines of evidence that indicate the RNase domain is dispensable for replication stress response and degradation of stalled replication forks. The equivalent RNase domain mutants in SLFN13 are shown to be deficient in tRNA cleavage[112]. The effect of the knockdown of nucleases DNA2 and MRE11 on fork degradation were similar in both cells expressing wild-type and the RNase deficient mutant SLFN11. However, unexpectedly, I also observed clearly reduced ATR protein expression in cells transduced with wild-type and RNase mutant SLFN11. The observed down-regulation of ATR protein levels cannot be explained by the SLFN11 cleavage of tRNA and translational control of ATR. This is in sharp contrast to the conclusion described in[111], which implicates SLFN11-mediated tRNA cleavage is responsible for ATR downregulation. The reason for this discrepancy is unclear and could be due to the use of different cell lines and methods. More experiments are needed to resolve this contradiction.

I propose that low ATR expression levels should contribute to the mechanism involved in increased DNA damage sensitivity mediated by SLFN11, at least in some cell lines. The decreased ATR expression or activity may account for many, if not all, properties conferred by SLFN11 expression. For example, it has been described that ATRi can

decrease homologous recombination repair, RAD51 foci accumulation, and DNA damage tolerance[111], and these are also the features of SLFN11 expressing cells. In our HAP1 cell models, I observed that ATRi treatment phenocopied SLFN11 exogenous expression in accelerating stalled fork degradation. The fork remodeling enzyme SMARCAL1 can be inhibited by ATR, and ATRi treatment may accelerate fork reversal[48] possibly contributing to increased fork degradation. This view is also consistent with the previous suggestion that ATRi can reverse chemoresistance caused by the loss of SLFN11[65,109,111].

At this moment, it is unclear whether the SLFN11-induced reduction of ATR protein levels universally occurs or not, and it is possible that the reduction of the ATR protein is a phenomenon observable only in a cell type-specific or context-specific manner. I could not detect ATR downregulation in HAP1 wild-type cells (expressing SLFN11) post-HU (4 mM, 5h). As reported by Li et al.[111], at least some cell lines have decreased ATR levels after camptothecin treatment (i.e., FG cells or HEK293 cells, 40 nM CPT for 24 or 48 h). Different cell lines may display different dose-response and kinetics in the regulation of ATR levels. A more thorough investigation would be warranted to examine whether SLFN11 can affect ATR levels in other cancer cell lines.

It is also currently unclear how the SLFN11 wild-type and RNase mutant can reduce protein levels of ATR. It has been described that SLFN11 can interact with DDB1 of CUL4 E3 ubiquitin ligase, promoting polyubiquitination and destabilization of a replication initiation factor CDT1[110]. This is shown to require the SLFN11 C-terminal helicase domain. The same or similar mechanism might be operating to reduce ATR expression levels, and this hypothesis can be tested in the future. In any case, my data did

not support the idea that SLFN11 RNase activity contributes to cell fate decisions following cancer chemotherapy.

Chapter 4 Discussion and conclusion

To maintain genome integrity, mammalian cells have developed intricate cellular response including DNA damage response, replication stress response as well as oxidative stress response. In this thesis, I have examined role of FXR1 in ROS-mediated ATM activation as well as the impact of the SLFN11 RNase domain on replication stress response via ATR kinase. Since defective cellular response leads to disorders, such as neurodegeneration disorder and cancer, my study shed some light on understanding not only the mechanism of how disease progress but also development of a novel disease treatment.

In chapter 2, I hypothesized that MRE11, the ATLD-responsible gene product may function in oxidative stress. ATLD patients show a similar neurodegeneration phenotype as A-T, such as progressive cerebellar ataxia. ATM, a protein product of A-T responsible gene, is activated in response to H_2O_2-induced oxidative stress. Using ATLD patient-derived cells lacking MRE11 function, I revealed that MRE11 is involved in the regulate on of ATM activation in response to oxidative stress. I further identified FXR1, a novel protein that binds to MRE11 by mass spectrometry. Finally, I clarified that independent of NBS1 and ATM, FXR1 forms a complex with MRE11 in the mitochondria and plays a role in cellular responses to oxidative stress. It has been reported that MRE11 localize in mitochondria and binds with mitochondria DNA[122]. In addition, MRE11 functions as a mitochondria protector, regulate activation of caspase 1 and prevent T cell death and inflammation[123]. Function of FXR1 in mitochondria DNA protection against oxidative stress should be investigated in the future.

In chapter 3, I investigated the function of SLFN11, a member of the long-form SLFNs that harbor the N-terminal ribonuclease (RNase) domain and the C-terminal helicase/ATPase domain. How these domains contribute to the chemotherapeutic response remains poorly understood. I tested whether SLFN11 mutated on RNase domain can affect replication stress response. I found that the RNase domain mutant was still able to suppress DNA damage tolerance and destabilize the stalled replication forks. The fork degradation is dependent on both DNA2 and MRE11 nuclease, but not on MRE11's novel interactor FXR1. This was not unexpected since FXR1 is expressed in cytoplasm or in mitochondria and may not have a nuclear function. It is interesting to note that MRE11 can exert both nuclear and cytoplasmic function, perhaps changing interaction partners (the MRE11-NBS1-RAD50 complex in the nucleus versus the MRE11-FXR1 complex in mitochondria). It remains unclear how MRE11 assists ATM in response to ROS and this will be an important issue to elucidate the mechanism.

Unexpectedly, SLFN11 expression downregulated the protein levels of ATR kinase, raising a possibility that the impact of SLFN11 expression on replication stress response is mediated by the reduced ATR protein levels. I also clarified that ATR inhibitor treatment accelerated the stalled fork degradation, consistent with the possible role of ATR in regulation of the fork reversal enzymes and/or in recruitment of the fork protection factors. Collectively, these results may suggest that a critical role of SLFN11 in cancer chemotherapy may involve the regulation of ATR levels. However, how SLFN11 affects protein levels of ATR remains unclear. Clarifying this would be an important research goal in near future. SLFN11 still may have a more direct role in prevention of RAD51 and other fork protector recruitment.

Inhibition of transcription due to damage in the template DNA or the replication-transcription conflicts form R-loops, which lead to genomic instability by increasing replication stress and inhibiting transcription. Thus, replication stress can further increase replication stress in a positive feedback mechanism. Besides its role in DNA damage responses and oxidative stress responses, MRE11 has been reported to function in suppressing R-loop formation via the Fanconi anemia pathway[98]. On the other hand, it has also been reported that ATR activated by replication stress promotes the localization of the RNA helicase Ddx19 to the cell nucleus and functions to clear the R-loop[124]. I have found that FXR1 is a novel MRE11's interactor, while whether FXR1 function in R-loop remains be investigated. It has been reported that SLFN11 interacts with DHX9 helicase, which may function in regulating R-loops[125]. I also demonstrated that SLFN11 could regulate ATR expression and function. Taken these together, the role of SLFN11 and FXR1 in regulating R-loop need to be further investigated.

In conclusion, the function analyses of FXR1 and SLFN11 described here provide a new insight to further understand the mechanism of cellular response to genotoxic stress, and possibly contribute to developments in the treatment of human disease, such as cancer and neurodegenerative disorder.

Reference

[1] A. Tubbs and A. Nussenzweig, “Endogenous DNA Damage as a Source of Genomic Instability in Cancer,” *Cell*, vol. 168, no. 4. Cell Press, pp. 644–656, Feb. 09, 2017. doi: 10.1016/j.cell.2017.01.002.

[2] P. H. N. Aguiar *et al.*, “Oxidative Stress and DNA Lesions: The Role of 8-Oxoguanine Lesions in Trypanosoma cruzi Cell Viability,” *PLoS Negl Trop Dis*, vol. 7, no. 6, 2013, doi: 10.1371/journal.pntd.0002279.

[3] N. P. Degtyareva, L. Heyburn, J. Sterling, M. A. Resnick, D. A. Gordenin, and P. W. Doetsch, “Oxidative stress-induced mutagenesis in single-strand DNA occurs primarily at cytosines and is DNA polymerase zeta-dependent only for adenines and guanines,” *Nucleic Acids Res*, vol. 41, no. 19, pp. 8995–9005, Oct. 2013, doi: 10.1093/nar/gkt671.

[4] P. Lin, V. K. Batra, L. C. Pedersen, W. A. Beard, S. H. Wilson, and L. G. Pedersen, “Incorrect nucleotide insertion at the active site of a G:A mismatch catalyzed by DNA polymerase β,” *Proceedings of the National Academy of Sciences*, vol. 105, no. 15, pp. 5670–5674, Apr. 2008, doi: 10.1073/pnas.0801257105.

[5] K. Valerie *et al.*, “Radiation-induced cell signaling: Inside-out and outside-in,” *Molecular Cancer Therapeutics*, vol. 6, no. 3. pp. 789–801, Mar. 2007. doi: 10.1158/1535-7163.MCT-06-0596.

[6] J. Nuszkiewicz, A. Woźniak, and K. Szewczyk-Golec, “Ionizing radiation as a source of oxidative stress—the protective role of melatonin and vitamin d,” *International Journal of Molecular Sciences*, vol. 21, no. 16. MDPI AG, pp. 1–22, Aug. 02, 2020. doi: 10.3390/ijms21165804.

[7] H. Tominaga, S. Kodama, N. Matsuda, K. Suzuki, and M. Watanabe, “Involvement of Reactive Oxygen Species (ROS) in the Induction of Genetic Instability by Radiation,” *J Radiat Res*, vol. 45, no. 2, pp. 181–188, Jun. 2004, doi: 10.1269/jrr.45.181.

[8] H. Masai, S. Matsumoto, Z. You, N. Yoshizawa-Sugata, and M. Oda, “Eukaryotic chromosome DNA replication: Where, when, and how?,” *Annual Review of Biochemistry*, vol. 79. pp. 89–130, Jul. 07, 2010. doi: 10.1146/annurev.biochem.052308.103205.

[9] N. Mailand, I. Gibbs-Seymour, and S. Bekker-Jensen, “Regulation of PCNA-protein interactions for genome stability,” *Nature Reviews Molecular Cell Biology*, vol. 14, no. 5. pp. 269–282, May 2013. doi: 10.1038/nrm3562.

[10] J. Z. Dalgaard, “Causes and consequences of ribonucleotide incorporation into nuclear DNA,” *Trends in Genetics*, vol. 28, no. 12. pp. 592–597, Dec. 2012. doi: 10.1016/j.tig.2012.07.008.

[11] A. Aguilera and T. García-Muse, “R Loops: From Transcription Byproducts to Threats to Genome Stability,” *Molecular Cell*, vol. 46, no. 2. pp. 115–124, Apr. 27, 2012. doi: 10.1016/j.molcel.2012.04.009.

[12] J. C. Saldivar *et al.*, “Initiation of Genome Instability and Preneoplastic Processes through Loss of Fhit Expression,” *PLoS Genet*, vol. 8, no. 11, Nov. 2012, doi: 10.1371/journal.pgen.1003077.

[13] A. C. Bester *et al.*, “Nucleotide deficiency promotes genomic instability in early stages of cancer development,” *Cell*, vol. 145, no. 3, pp. 435–446, Apr. 2011, doi: 10.1016/j.cell.2011.03.044.

[14] K. K. Khanna and S. P. Jackson, “DNA double-strand breaks: signaling, repair and the cancer connection,” *Nat Genet*, vol. 27, no. 3, pp. 247–254, 2001, doi: 10.1038/85798.

[15] M. K. Zeman and K. A. Cimprich, “R E V I E W Causes and consequences of replication stress,” 2014.

[16] W. Yang, “Structure and mechanism for DNA lesion recognition,” *Cell Res*, vol. 18, no. 1, pp. 184–197, Jan. 2008, doi: 10.1038/cr.2007.116.

[17] K. Finn, N. F. Lowndes, and M. Grenon, “Eukaryotic DNA damage checkpoint activation in response to double-strand breaks,” *Cellular and Molecular Life Sciences*, vol. 69, no. 9. pp. 1447–1473, May 2012. doi: 10.1007/s00018-011-0875-3.

[18] C. Redon, D. Pilch, E. Rogakou, O. Sedelnikova, K. Newrock, and W. Bonner, “Histone H2A variants H2AX and H2AZ,” *Curr Opin Genet Dev*, vol. 12, no. 2, pp. 162–169, 2002, doi: https://doi.org/10.1016/S0959-437X(02)00282-4.

[19] L. J. Kuo and L. X. Yang, “γ-H2AX- A novel biomaker for DNA double-strand breaks,” *In Vivo (Brooklyn)*, vol. 22, no. 3, pp. 305–310, 2008.

[20] M. Podhorecka, A. Skladanowski, and P. Bozko, “H2AX phosphorylation: Its role in DNA damage response and cancer therapy,” *Journal of Nucleic Acids*, vol. 2010. 2010. doi: 10.4061/2010/920161.

[21] S. Burma, B. P. C. Chen, and D. J. Chen, “Role of non-homologous end joining (NHEJ) in maintaining genomic integrity,” *DNA Repair*, vol. 5, no. 9–10. pp. 1042–1048, Sep. 08, 2006. doi: 10.1016/j.dnarep.2006.05.026.

[22] J. San Filippo, P. Sung, and H. Klein, “Mechanism of eukaryotic homologous recombination,” *Annual Review of Biochemistry*, vol. 77. pp. 229–257, 2008. doi: 10.1146/annurev.biochem.77.061306.125255.

[23] M. L. Hefferin and A. E. Tomkinson, “Mechanism of DNA double-strand break repair by non-homologous end joining,” *DNA Repair*, vol. 4, no. 6. Elsevier, pp. 639–648, Jun. 08, 2005. doi: 10.1016/j.dnarep.2004.12.005.

[24] A. Sallmyr, J. Fan, and F. V. Rassool, “Genomic instability in myeloid malignancies: Increased reactive oxygen species (ROS), DNA double strand breaks (DSBs) and error-prone repair,” *Cancer Letters*, vol. 270, no. 1. Elsevier Ireland Ltd, pp. 1–9, Oct. 18, 2008. doi: 10.1016/j.canlet.2008.03.036.

[25] A. v. Nimonkar *et al.*, “BLM-DNA2-RPA-MRN and EXO1-BLM-RPA-MRN constitute two DNA end resection machineries for human DNA break repair,” *Genes Dev*, vol. 25, no. 4, pp. 350–362, Feb. 2011, doi: 10.1101/gad.2003811.

[26] M. D. Adams, M. McVey, and J. J. Sekelsky, “Drosophila BLM in double-strand break repair by synthesis-dependent strand annealing,” *Science (1979)*, vol. 299, no. 5604, pp. 265–267, Jan. 2003, doi: 10.1126/science.1077198.

[27] A. H. Bizard and I. D. Hickson, “The Dissolution of Double Holliday Junctions.” Accessed: Sep. 16, 2022. [Online]. Available: doi: 10.1101/cshperspect.a016477

[28] S. P. Jackson and J. Bartek, “The DNA-damage response in human biology and disease,” *Nature*, vol. 461, no. 7267, pp. 1071–1078, 2009, doi: 10.1038/nature08467.

[29] M. Shrivastav, L. P. de Haro, and J. A. Nickoloff, “Regulation of DNA double-strand break repair pathway choice,” *Cell Res*, vol. 18, no. 1, pp. 134–147, Jan. 2008, doi: 10.1038/cr.2007.111.

[30] M. Kastan and C. Bakkenist, “DNA damage activates ATM through intermolecular autophosphorylation and dimmer association,” *Nature*, vol. 421, pp. 499–506, 2003.

[31] J. H. Lee and T. T. Paull, “Activation and regulation of ATM kinase activity in response to DNA double-strand breaks,” *Oncogene*, vol. 26, no. 56. pp. 7741–7748, Dec. 10, 2007. doi: 10.1038/sj.onc.1210872.

[32] K. Savitsky *et al.*, “A single ataxia telangiectasia gene with a product similar to PI-3 kinase,” *Science (1979)*, vol. 268, no. 5218, pp. 1749–1753, 1995, doi: 10.1126/science.7792600.

[33] Z. Guo, S. Kozlov, M. F. Lavin, M. D. Person, and T. T. Paull, “ATM Activation by Oxidative Stress,” *Science (1979)*, vol. 330, no. 6003, pp. 517–521, Oct. 2010, doi: 10.1126/science.1192912.

[34] A. N. Blackford and S. P. Jackson, “ATM, ATR, and DNA-PK: The Trinity at the Heart of the DNA Damage Response,” *Molecular Cell*, vol. 66, no. 6. Cell Press, pp. 801–817, Jun. 15, 2017. doi: 10.1016/j.molcel.2017.05.015.

[35] J. C. Saldivar, D. Cortez, and K. A. Cimprich, “The essential kinase ATR: Ensuring faithful duplication of a challenging genome,” *Nat Rev Mol Cell Biol*, vol. 18, no. 10, pp. 622–636, 2017, doi: 10.1038/nrm.2017.67.

[36] A. Kumagai, J. Lee, H. Y. Yoo, and W. G. Dunphy, “TopBP1 activates the ATR-ATRIP complex,” *Cell*, vol. 124, no. 5, pp. 943–955, Mar. 2006, doi: 10.1016/j.cell.2005.12.041.

[37] J. Bartek and J. Lukas, “Chk1 and Chk2 kinases in checkpoint control and cancer,” *Cancer Cell*, vol. 3, no. 5, pp. 421–429, 2003, doi: 10.1016/S1535-6108(03)00110-7.

[38] J. C. Saldivar, D. Cortez, and K. A. Cimprich, “The essential kinase ATR: Ensuring faithful duplication of a challenging genome,” *Nature Reviews Molecular Cell Biology*, vol. 18, no. 10. Nature Publishing Group, pp. 622–636, Oct. 01, 2017. doi: 10.1038/nrm.2017.67.

[39] A. M. Woodward *et al.*, “Excess Mcm2-7 license dormant origins of replication that can be used under conditions of replicative stress,” *Journal of Cell Biology*, vol. 173, no. 5, pp. 673–683, Jun. 2006, doi: 10.1083/jcb.200602108.

[40] D. McIntosh and J. J. Blow, “Dormant origins, the licensing checkpoint, and the response to replicative stresses,” *Cold Spring Harb Perspect Biol*, vol. 4, no. 10, Oct. 2012, doi: 10.1101/cshperspect.a012955.

[41] X. Q. Ge, D. A. Jackson, and J. J. Blow, “Dormant origins licensed by excess Mcm2-7 are required for human cells to survive replicative stress,” *Genes Dev*, vol. 21, no. 24, pp. 3331–3341, Dec. 2007, doi: 10.1101/gad.457807.

[42] M. Lopes, M. Foiani, and J. M. Sogo, “Multiple Mechanisms Control Chromosome Integrity after Replication Fork Uncoupling and Restart at Irreparable UV Lesions,” *Mol Cell*, vol. 21, no. 1, pp. 15–27, 2006, doi: https://doi.org/10.1016/j.molcel.2005.11.015.

[43] I. Elvers, F. Johansson, P. Groth, K. Erixon, and T. Helleday, “UV stalled replication forks restart by re-priming in human fibroblasts,” *Nucleic Acids Res*, vol. 39, no. 16, pp. 7049–7057, Sep. 2011, doi: 10.1093/nar/gkr420.

[44] J. Hu *et al.*, “The Intra-S Phase Checkpoint Targets Dna2 to Prevent Stalled Replication Forks from Reversing,” *Cell*, vol. 149, no. 6, pp. 1221–1232, 2012, doi: https://doi.org/10.1016/j.cell.2012.04.030.

[45] J. M. Sogo, M. Lopes, and M. Foiani, “Fork Reversal and ssDNA Accumulation at Stalled Replication Forks Owing to Checkpoint Defects,” *Science (1979)*, vol. 297, no. 5581, pp. 599–602, Jul. 2002, doi: 10.1126/science.1074023.

[46] C. Cotta-Ramusino *et al.*, “Exo1 Processes Stalled Replication Forks and Counteracts Fork Reversal in Checkpoint-Defective Cells,” *Mol Cell*, vol. 17, no. 1, pp. 153–159, 2005, doi: https://doi.org/10.1016/j.molcel.2004.11.032.

[47] J. Hu *et al.*, “The Intra-S Phase Checkpoint Targets Dna2 to Prevent Stalled Replication Forks from Reversing,” *Cell*, vol. 149, no. 6, pp. 1221–1232, 2012, doi: https://doi.org/10.1016/j.cell.2012.04.030.

[48] F. B. Couch *et al.*, “ATR phosphorylates SMARCAL1 to prevent replication fork collapse,” *Genes Dev*, vol. 27, no. 14, pp. 1610–1623, Jul. 2013, doi: 10.1101/gad.214080.113.

[49] A. Ray Chaudhuri *et al.*, “Topoisomerase i poisoning results in PARP-mediated replication fork reversal,” *Nat Struct Mol Biol*, vol. 19, no. 4, pp. 417–423, Apr. 2012, doi: 10.1038/nsmb.2258.

[50] A. M. R. Taylor, Z. Lam, J. I. Last, and P. J. Byrd, “Ataxia telangiectasia: More variation at clinical and cellular levels,” *Clin Genet*, vol. 87, no. 3, pp. 199–208, 2015, doi: 10.1111/cge.12453.

[51] N. Gueven *et al.*, “A subgroup of spinocerebellar ataxias defective in DNA damage responses,” *Neuroscience*, vol. 145, no. 4, pp. 1418–1425, 2007, doi: 10.1016/j.neuroscience.2006.12.010.

[52] T. Ogi *et al.*, “Identification of the First ATRIP-Deficient Patient and Novel Mutations in ATR Define a Clinical Spectrum for ATR-ATRIP Seckel Syndrome,” *PLoS Genet*, vol. 8, no. 11, Nov. 2012, doi: 10.1371/journal.pgen.1002945.

[53] M. Murga *et al.*, “A mouse model of ATR-Seckel shows embryonic replicative stress and accelerated aging,” *Nat Genet*, vol. 41, no. 8, pp. 891–898, Aug. 2009, doi: 10.1038/ng.420.

[54] M. O’Driscoll and P. A. Jeggo, “The role of the DNA damage response pathways in brain development and microcephaly: Insight from human disorders,” *DNA Repair (Amst)*, vol. 7, no. 7, pp. 1039–1050, 2008, doi: https://doi.org/10.1016/j.dnarep.2008.03.018.

[55] E. Seemanová and P. Jarolím, “Nijmegen breakage syndrom (NBS),” *Cesk Pediatr*, vol. 54, no. 2, pp. 97–101, 1999, doi: 10.1186/1750-1172-7-13.

[56] A. M. R. Taylor, A. Groom, and P. J. Byrd, “Ataxia-telangiectasia-like disorder (ATLD)—its clinical presentation and molecular basis,” *DNA Repair (Amst)*, vol. 3, no. 8, pp. 1219–1225, 2004, doi: https://doi.org/10.1016/j.dnarep.2004.04.009.

[57] M. R. Stratton, P. J. Campbell, and P. A. Futreal, “The cancer genome,” *Nature*, vol. 458, no. 7239. pp. 719–724, Apr. 09, 2009. doi: 10.1038/nature07943.

[58] M. S. Schlissel, C. R. Kaffer, and J. D. Curry, “Leukemia and lymphoma: A cost of doing business for adaptive immunity,” *Genes and Development*, vol. 20, no. 12. pp. 1539–1544, Jun. 15, 2006. doi: 10.1101/gad.1446506.

[59] C. H. Bassing and F. W. Alt, “The cellular response to general and programmed DNA double strand breaks,” *DNA Repair (Amst)*, vol. 3, no. 8, pp. 781–796, 2004, doi: https://doi.org/10.1016/j.dnarep.2004.06.001.

[60] J. Jiricny, “The multifaceted mismatch-repair system,” *Nature Reviews Molecular Cell Biology*, vol. 7, no. 5. pp. 335–346, May 2006. doi: 10.1038/nrm1907.

[61] C. Lengauer and K. W. Kinzler, “Genetic instabilities in human cancers,” 1998. [Online]. Available: www.nature.com

[62] A. Rotte, “Combination of CTLA-4 and PD-1 blockers for treatment of cancer,” *Journal of Experimental and Clinical Cancer Research*, vol. 38, no. 1. BioMed Central Ltd., Jun. 13, 2019. doi: 10.1186/s13046-019-1259-z.

[63] S. Dasari and P. Bernard Tchounwou, “Cisplatin in cancer therapy: Molecular mechanisms of action,” *European Journal of Pharmacology*, vol. 740. Elsevier, pp. 364–378, Oct. 05, 2014. doi: 10.1016/j.ejphar.2014.07.025.

[64] M. J. O’Connor, “Targeting the DNA Damage Response in Cancer,” *Molecular Cell*, vol. 60, no. 4. Cell Press, pp. 547–560, Nov. 19, 2015. doi: 10.1016/j.molcel.2015.10.040.

[65] J. Murai *et al.*, “Resistance to PARP inhibitors by SLFN11 inactivation can be overcome by ATR inhibition,” *Oncotarget*, vol. 7, no. 47, pp. 76534–76550, 2016, doi: 10.18632/oncotarget.12266.

[66] U. Jo *et al.*, “SLFN11 promotes CDT1 degradation by CUL4 in response to replicative DNA damage, while its absence leads to synthetic lethality with ATR/CHK1 inhibitors,” *Proc Natl Acad Sci U S A*, vol. 118, no. 6, pp. 1–12, 2021, doi: 10.1073/pnas.2015654118.

[67] G. Zoppoli *et al.*, “Putative DNA/RNA helicase Schlafen-11 (SLFN11) sensitizes cancer cells to DNA-damaging agents,” *Proc Natl Acad Sci U S A*, vol. 109, no. 37, pp. 15030–15035, Sep. 2012, doi: 10.1073/pnas.1205943109.

[68] S. Al-Marsoummi, E. E. Vomhof-Dekrey, and M. D. Basson, “Schlafens: Emerging proteins in cancer cell biology,” *Cells*, vol. 10, no. 9. MDPI, Sep. 01, 2021. doi: 10.3390/cells10092238.

[69] T. T. Paull, “Mechanisms of ATM activation,” *Annual Review of Biochemistry*, vol. 84. Annual Reviews Inc., pp. 711–738, Jun. 02, 2015. doi: 10.1146/annurev-biochem-060614-034335.

[70] J. Kobayashi, “Ataxia-Telangiectasia and Nijmegen Breakage Syndrome,” in *DNA Repair Disorders*, C. Nishigori and K. Sugasawa, Eds. Singapore: Springer Singapore, 2019, pp. 191–201. doi: 10.1007/978-981-10-6722-8_13.

[71] A. Jazayeri *et al.*, “ATM- and cell cycle-dependent regulation of ATR in response to DNA double-strand breaks,” *Nat Cell Biol*, vol. 8, no. 1, pp. 37–45, 2006, doi: 10.1038/ncb1337.

[72] R. B. Painter and B. R. Young, “Radiosensitivity in ataxia-telangiectasia: A new explanation,” *Proc Natl Acad Sci U S A*, vol. 77, no. 12 II, pp. 7315–7317, 1980, doi: 10.1073/pnas.77.12.7315.

[73] N. Gueven *et al.*, “A subgroup of spinocerebellar ataxias defective in DNA damage responses,” *Neuroscience*, vol. 145, no. 4. pp. 1418–1425, Apr. 14, 2007. doi: 10.1016/j.neuroscience.2006.12.010.

[74] H. Date *et al.*, “Early-onset ataxia with ocular motor apraxia and hypoalbuminemia is caused by mutations in a new HIT superfamily gene,” 2001. [Online]. Available: http://www.sanger.ac.uk/HGP/Chr9/

[75] I. Ahel *et al.*, “The neurodegenerative disease protein aprataxin resolves abortive DNA ligation intermediates,” *Nature*, vol. 443, no. 7112, pp. 713–716, Oct. 2006, doi: 10.1038/nature05164.

[76] M. Groh, L. O. Albulescu, A. Cristini, and N. Gromak, “Senataxin: Genome Guardian at the Interface of Transcription and Neurodegeneration,” *Journal of Molecular Biology*, vol. 429, no. 21. Academic Press, pp. 3181–3195, Oct. 27, 2017. doi: 10.1016/j.jmb.2016.10.021.

[77] N. A. A. Murad *et al.*, “Mitochondrial dysfunction in a novel form of autosomal recessive ataxia,” *Mitochondrion*, vol. 13, no. 3. pp. 235–245, May 2013. doi: 10.1016/j.mito.2012.11.006.

[78] J. Kobayashi, Y. Saito, M. Okui, N. Miwa, and K. Komatsu, “Increased oxidative stress in AOA3 cells disturbs ATM-dependent DNA damage responses,” *Mutat Res Genet Toxicol Environ Mutagen*, vol. 782, pp. 42–50, Apr. 2015, doi: 10.1016/j.mrgentox.2015.03.012.

[79] N. Stern *et al.*, “Accumulation of DNA damage and reduced levels of nicotine adenine dinucleotide in the brains of Atm-deficient mice,” *Journal of Biological Chemistry*, vol. 277, no. 1, pp. 602–608, Jan. 2002, doi: 10.1074/jbc.M106798200.

[80] A. Kamsler *et al.*, “Increased oxidative stress in ataxia telangiectasia evidenced by alterations in redox state of brains from Atm-deficient mice,” *Cancer Res*, vol. 61, no. 5, pp. 1849–1854, 2001.

[81] Y. A. Valentin-Vega *et al.*, “Mitochondrial dysfunction in ataxia-telangiectasia,” *Blood*, vol. 119, no. 6, pp. 1490–1500, 2012, doi: 10.1182/blood-2011-08-373639.

[82] J.-H. Lee and T. T. Paull, “ATM Activation by DNA Double-Strand Breaks Through the Mre11-Rad50-Nbs1 Complex,” 2005. [Online]. Available: www.sciencemag.org

[83] T. Yoshida *et al.*, “Hypergonadotropic hypogonadism and hypersegmented neutrophils in a patient with ataxia-telangiectasia-like disorder: Potential diagnostic clues?,” *Am J Med Genet A*, vol. 164, no. 7, pp. 1830–1834, 2014, doi: 10.1002/ajmg.a.36546.

[84] H. Tauchi *et al.*, “The forkhead-associated domain of NBS1 is essential for nuclear foci formation after irradiation but not essential for hRAD50·hMRE11·-NBS1 complex DNA repair activity,” *Journal of Biological Chemistry*, vol. 276, no. 1, pp. 12–15, Jan. 2001, doi: 10.1074/jbc.C000578200.

[85] T. Kondo *et al.*, “DNA damage sensor MRE11 recognizes cytosolic double-stranded DNA and induces type i interferon by regulating STING trafficking,” *Proc Natl Acad Sci U S A*, vol. 110, no. 8, pp. 2969–2974, Feb. 2013, doi: 10.1073/pnas.1222694110.

[86] A. Kamsler *et al.*, “Increased Oxidative Stress in Ataxia Telangiectasia Evidenced by Alterations in Redox State of Brains from Atm-deficient Mice 1,” 2001. [Online]. Available: http://aacrjournals.org/cancerres/article-pdf/61/5/1849/2491519/ch050101849.pdf

[87] N. Stern *et al.*, “Accumulation of DNA damage and reduced levels of nicotine adenine dinucleotide in the brains of Atm-deficient mice,” *Journal of Biological Chemistry*, vol. 277, no. 1, pp. 602–608, Jan. 2002, doi: 10.1074/jbc.M106798200.

[88] D. Oba *et al.*, “Autopsy study of cerebellar degeneration in siblings with ataxia-telangiectasia-like disorder,” *Acta Neuropathol*, vol. 119, no. 4, pp. 513–520, Apr. 2010, doi: 10.1007/s00401-010-0639-4.

[89] M. C. Siomi, H. Siomi, W. H. Sauer, S. Srinivasan1, R. L. Nussbaum1, and G. Dreyfuss2, “FXR1, an autosomal homolog of the fragile X mental retardation gene,” 1995.

[90] E. Say *et al.*, “A Functional Requirement for PAK1 Binding to the KH(2) Domain of the Fragile X Protein-Related FXR1,” *Mol Cell*, vol. 38, no. 2, pp. 236–249, Apr. 2010, doi: 10.1016/j.molcel.2010.04.004.

[91] X. Wang *et al.*, “Cdc42-dependent activation of NADPH oxidase is involved in Ethanol-Induced neuronal oxidative stress,” *PLoS One*, vol. 7, no. 5, May 2012, doi: 10.1371/journal.pone.0038075.

[92] F. Bodaleo, C. Tapia-Monsalves, C. Cea-Del Rio, C. Gonzalez-Billault, and A. Nunez-Parra, “Structural and functional abnormalities in the olfactory system of fragile x syndrome models,” *Frontiers in Molecular Neuroscience*, vol. 12. Frontiers Media S.A., May 27, 2019. doi: 10.3389/fnmol.2019.00135.

[93] M. Shen *et al.*, “Reduced mitochondrial fusion and Huntingtin levels contribute to impaired dendritic maturation and behavioral deficits in Fmr1-mutant mice,” *Nat Neurosci*, vol. 22, no. 3, pp. 386–400, Mar. 2019, doi: 10.1038/s41593-019-0338-y.

[94] E. Fernández and F. A. Mallette, “The Rise of FXR1: Escaping Cellular Senescence in Head and Neck Squamous Cell Carcinoma,” *PLoS Genet*, vol. 12, no. 11, Nov. 2016, doi: 10.1371/journal.pgen.1006344.

[95] M. Majumder *et al.*, “RNA-Binding Protein FXR1 Regulates p21 and TERC RNA to Bypass p53-Mediated Cellular Senescence in OSCC,” *PLoS Genet*, vol. 12, no. 9, Sep. 2016, doi: 10.1371/journal.pgen.1006306.

[96] N. E. Patzlaff, K. M. Nemec, S. G. Malone, Y. Li, and X. Zhao, “Fragile X related protein 1 (FXR1P) regulates proliferation of adult neural stem cells,” *Hum Mol Genet*, vol. 26, no. 7, pp. 1340–1352, Apr. 2017, doi: 10.1093/hmg/ddx034.

[97] T. García-Muse and A. Aguilera, “R Loops: From Physiological to Pathological Roles,” *Cell*, vol. 179, no. 3. Cell Press, pp. 604–618, Oct. 17, 2019. doi: 10.1016/j.cell.2019.08.055.

[98] E. Y. C. Chang *et al.*, “MRE11-RAD50-NBS1 promotes Fanconi Anemia R-loop suppression at transcription–replication conflicts,” *Nat Commun*, vol. 10, no. 1, Dec. 2019, doi: 10.1038/s41467-019-12271-w.

[99] D. A. Schwarz, C. D. Katayama, and S. M. Hedrick, “Schlafen, a new family of growth regulatory genes that affect thymocyte development,” *Immunity*, vol. 9, no. 5, pp. 657–668, 1998, doi: 10.1016/S1074-7613(00)80663-9.

[100] O. Bustos *et al.*, “Evolution of the Schlafen genes, a gene family associated with embryonic lethality, meiotic drive, immune processes and orthopoxvirus virulence,” *Gene*, vol. 447, no. 1, pp. 1–11, 2009, doi: 10.1016/j.gene.2009.07.006.

[101] F. Liu, P. Zhou, Q. Wang, M. Zhang, and D. Li, “The Schlafen family: complex roles in different cell types and virus replication,” *Cell Biol Int*, vol. 42, no. 1, pp. 2–8, 2018, doi: 10.1002/cbin.10778.

[102] U. Jo and Y. Pommier, “Structural, molecular, and functional insights into Schlafen proteins,” *Exp Mol Med*, vol. 54, no. 6, pp. 730–738, 2022, doi: 10.1038/s12276-022-00794-0.

[103] G. Zoppoli *et al.*, “Putative DNA/RNA helicase Schlafen-11 (SLFN11) sensitizes cancer cells to DNA-damaging agents,” *Proc Natl Acad Sci U S A*, vol. 109, no. 37, pp. 15030–15035, 2012, doi: 10.1073/pnas.1205943109.

[104] B. Zhang *et al.*, “A wake-up call for cancer DNA damage: the role of Schlafen 11 (SLFN11) across multiple cancers,” *Br J Cancer*, vol. 125, no. 10, pp. 1333–1340, 2021, doi: 10.1038/s41416-021-01476-w.

[105] F. G. Sousa *et al.*, “Alterations of DNA repair genes in the NCI-60 cell lines and their predictive value for anticancer drug activity,” *DNA Repair (Amst)*, vol. 28, pp. 107–115, Apr. 2015, doi: 10.1016/j.dnarep.2015.01.011.

[106] M. Berti, D. Cortez, and M. Lopes, “The plasticity of DNA replication forks in response to clinically relevant genotoxic stress,” *Nat Rev Mol Cell Biol*, vol. 21, no. 10, pp. 633–651, 2020, doi: 10.1038/s41580-020-0257-5.

[107] Y. Okamoto *et al.*, “SLFN11 promotes stalled fork degradation that underlies the phenotype in Fanconi anemia cells,” *Blood*, vol. 137, no. 3, pp. 336–348, Jan. 2021, doi: 10.1182/blood.2019003782.

[108] Y. Mu *et al.*, “ SLFN 11 inhibits checkpoint maintenance and homologous recombination repair ,” *EMBO Rep*, vol. 17, no. 1, pp. 94–109, Jan. 2016, doi: 10.15252/embr.201540964.

[109] J. Murai *et al.*, “SLFN11 Blocks Stressed Replication Forks Independently of ATR,” *Mol Cell*, vol. 69, no. 3, pp. 371-384.e6, Feb. 2018, doi: 10.1016/j.molcel.2018.01.012.

[110] U. Jo *et al.*, “SLFN11 promotes CDT1 degradation by CUL4 in response to replicative DNA damage, while its absence leads to synthetic lethality with ATR/CHK1 inhibitors”, doi: 10.1073/pnas.2015654118/-/DCSupplemental.

[111] M. Li, E. Kao, D. Malone, X. Gao, J. Y. J. Wang, and M. David, “DNA damage-induced cell death relies on SLFN11-dependent cleavage of distinct type II tRNAs,” *Nat Struct Mol Biol*, vol. 25, no. 11, pp. 1047–1058, Nov. 2018, doi: 10.1038/s41594-018-0142-5.

[112] J. Y. Yang *et al.*, “Structure of Schlafen13 reveals a new class of tRNA/rRNA-targeting RNase engaged in translational control,” *Nat Commun*, vol. 9, no. 1, Dec. 2018, doi: 10.1038/s41467-018-03544-x.

[113] M. Li *et al.*, “Codon-usage-based inhibition of HIV protein synthesis by human schlafen 11,” *Nature*, vol. 491, no. 7422, pp. 125–128, Nov. 2012, doi: 10.1038/nature11433.

[114] F. J. Metzner, S. J. Wenzl, M. Kugler, S. Krebs, K.-P. Hopfner, and K. Lammens, “Mechanistic understanding of human SLFN11,” *Nat Commun*, vol. 13, no. 1, p. 5464, Sep. 2022, doi: 10.1038/s41467-022-33123-0.

[115] F. J. Metzner, E. Huber, K. P. Hopfner, and K. Lammens, “Structural and biochemical characterization of human Schlafen 5,” *Nucleic Acids Res*, vol. 50, no. 2, pp. 1147–1161, Jan. 2022, doi: 10.1093/nar/gkab1278.

[116] F. Qi, Q. Meng, I. Hayashi, and J. Kobayashi, “FXR1 is a novel MRE11-binding partner and participates in oxidative stress responses,” *J Radiat Res*, vol. 61, no. 3, pp. 368–375, Apr. 2020, doi: 10.1093/jrr/rraa011.

[117] H. Kim *et al.*, “Combining PARP with ATR inhibition overcomes PARP inhibitor and platinum resistance in ovarian cancer models,” *Nat Commun*, vol. 11, no. 1, Dec. 2020, doi: 10.1038/s41467-020-17127-2.

[118] K. Rickman and A. Smogorzewska, “Advances in understanding DNA processing and protection at stalled replication forks,” *Journal of Cell Biology*, vol. 218, no. 4. Rockefeller University Press, pp. 1096–1107, 2019. doi: 10.1083/jcb.201809012.

[119] Y. Okamoto *et al.*, “SLFN11 promotes stalled fork degradation that underlies the phenotype in Fanconi anemia cells,” 2021. Accessed: Sep. 16, 2022. [Online]. Available: https://doi.org/10.1182/blood.2019003782

[120] S. Liu *et al.*, “ATR Autophosphorylation as a Molecular Switch for Checkpoint Activation,” *Mol Cell*, vol. 43, no. 2, pp. 192–202, Jul. 2011, doi: 10.1016/j.molcel.2011.06.019.

[121] S. Liu *et al.*, “Distinct roles for DNA-PK, ATM and ATR in RPA phosphorylation and checkpoint activation in response to replication stress,” *Nucleic Acids Res*, vol. 40, no. 21, pp. 10780–10794, 2012, doi: 10.1093/nar/gks849.

[122] N. I. Dmitrieva, D. Malide, and M. B. Burg, “Mre11 is expressed in mammalian mitochondria where it binds to mitochondrial DNA,” *American Journal of Physiology-Regulatory, Integrative and Comparative Physiology*, vol. 301, no. 3, pp. R632–R640, Jun. 2011, doi: 10.1152/ajpregu.00853.2010.

[123] Y. Li *et al.*, “The DNA Repair Nuclease MRE11A Functions as a Mitochondrial Protector and Prevents T Cell Pyroptosis and Tissue Inflammation,” *Cell Metab*, vol. 30, no. 3, pp. 477-492.e6, 2019, doi: https://doi.org/10.1016/j.cmet.2019.06.016.

[124] D. Hodroj *et al.*, " An ATR -dependent function for the Ddx19 RNA helicase in nuclear R-loop metabolism ," *EMBO J*, vol. 36, no. 9, pp. 1182–1198, May 2017, doi: 10.15252/embj.201695131.

[125] P. Chakraborty, J. T. J. Huang, and K. Hiom, "DHX9 helicase promotes R-loop formation in cells with impaired RNA splicing," *Nat Commun*, vol. 9, no. 1, Dec. 2018, doi: 10.1038/s41467-018-06677-1.

Acknowledgements

Approaching the end of an incredible journey, I want to express my gratitude to those who helped me generously, without them I won't be able to finish my study in Japan.

First, I would like to express my gratitude to my supervisors:

Professor Junya Kobayashi for giving me the opportunity to study in Kyoto University and very thanks for his design and guidance in the chapter 2 research, as well as providing the all support for my first paper submission. Thank for his valuable advices and support for my life and study in Japan.

Professor Minoru Takata, who provided so much support for my doctoral study. He is a diligent supervisor who is always being around in the laboratory for students. His hard-working attitude inspired me deeply. If I have any question in study, I can discuss with him anytime. With his constructive suggestions and comments, I could be a better person in research.

Asst. Prof. Anfeng Mu, who offered me so much support in my research. He taught me experimental procedure with patience, and he made sure that I've learned everything correctly too. I've been motivated to improving constantly my experimental techniques and analytical methods with his guidance.

I am very lucky to have such caring supervisors in my doctoral study, without them I can't complete my doctoral course.

I would also like to thank members of Takata Lab:

Dr. Yusuke Okamoto for preparing the HAP1 *SLFN11*$^{-/-}$ cells.

Ms. Erin Alvi cloned the SLFN11 cDNA and English editing in Chapter 3.

Ms. Minori Ogawa for cooperation in DNA fiber assay.

Masami Tanaka, Mayu Yamabe, Sumiko Matsui, Xuye Wang, and Mr. Lin Liu for technical and secretarial assistance.

I would also like to express my gratitude to Professor Kenshi Komatsu, Professor Hiroshi Harada, and Radiation Research Center of Kyoto University for providing me all of environment and equipment for my research.

I would like to express my gratitude to previously members in Radiation Research Center of Kyoto University: Dr. Yukiko Nakase, Mr. Masahiro Takado, Dr. Michiko Suma, Dr. Kasumi Kawamura for their kind help for my life and study in Japan.

In addition, I would like to thank financial support from the MEXT scholarship.

Finally, very special thanks to my parent, my fiancé, and friends for their loving consideration and great confidence in me all through these years in Japan.

Qi Fei

Graduate School of Human Environmental Studies

Kyoto University

Japan